

Deducing formation routes of oxylipins by quantitative multiple heart-cutting achiral-chiral 2D-LC-MS

Nadja Kampschulte, Rebecca Kirchhoff, Ariane Löwen, Nils Helge Schebb*

Chair of Food Chemistry, School of Mathematics and Natural Sciences, University of Wuppertal, 42119 Wuppertal, GERMANY

**corresponding author:*

Nils Helge Schebb

Chair of Food Chemistry, Faculty of Mathematics and Natural Sciences, University of Wuppertal
Gaussstrasse 20, 42119 Wuppertal, Germany

Email: nils@schebb-web.de

Phone: +49-202-439-3457

Abstract

Introduction: Several oxylipins are key regulators of inflammation. Those are formed by enzymes such as lipoxygenases or cyclooxygenases but also by autoxidation. While the autoxidation is stereorandom, only individual stereoisomers are formed enzymatically. Oxylipin formation is comprehensively analyzed by reversed-phase liquid chromatography-tandem mass spectrometry (LC-MS/MS) methods, simultaneously quantifying > 150 oxylipins including numerous positional isomers. Enantiomers are not separated and enantioselective methods lack sensitivity and selectivity.

Objectives: Development and application of a method enabling the sensitive, specific and enantioselective analysis of oxylipins allowing the investigation of the formation routes of hydroxy- and dihydroxy-fatty acids in biological samples.

Methods: An achiral-chiral multiple heart-cutting two-dimensional (2D)-LC-MS/MS method was developed. The separation of 45 pairs of enantiomeric hydroxy- and vicinal dihydroxy-fatty acids is achieved within 1.80 min with lower limits of quantification below 1 pg on column. Enantiomeric fractions of oxylipins can be precisely ($\pm 5\%$) determined even at low concentrations or high enantiomeric excess of one isomer. The method was applied on the analysis of oxylipins in human cells.

Results: In human M2-like macrophages, the so-called specialized pro-resolving mediators (SPM) 5,15-DiHEPE and 7,17-DiHDHA as well as 5,15-DiHETE occurred as (*S,S*)-enantiomer, supporting their enzymatic formation. In contrast, at least eight isomers of 10,17-DiHDHA are present in immune cells indicating formation by autoxidation. Consistent with the literature, in human plasma of healthy subjects these dihydroxy-fatty acids are not present. However, they quickly form by autoxidation if the samples are stored improperly, yielding all four stereoisomers.

Conclusion: Using the first two-dimensional liquid chromatography method for the quantitative analysis of oxylipins with chiral separation, we could show that not only the specific enantiomers of dihydroxy-PUFA described as SPM are present in biological samples but numerous isomers can be found. These are rapidly formed during inappropriate sample storage. Thus, dihydroxy-FA should only be reported as SPM if an enantioselective analysis has been carried out.

Introduction

Oxylipins are a heterogenic group of lipids derived from the oxidation of (poly-) unsaturated fatty acids. Several oxylipins are formed by non-enzymatic free radical reactions but the biosynthesis of oxylipins is catalyzed by lipoxygenases (LOX), cyclooxygenases (COX), or by cytochrome P450 monooxygenases (CYP). While the enzymatic pathways are highly stereo- and enantiospecific, the autoxidative pathways lead to stereorandom products [1, 2]. Many oxylipins are potent lipid mediators, regulating physiological processes such as blood coagulation, fever, inflammation and blood pressure. However, the physiological effects of lipid mediators are rarely attributed to single oxylipins, but rather to the shift in the oxylipin pattern. Therefore, liquid chromatography-tandem mass spectrometry (LC-MS/MS)-based multi-methods covering large numbers of structurally diverse oxylipins are state of the art for the investigation of lipid mediator biology [3-7]. These powerful reversed-phase (RP) chromatography methods are characterized by high selectivity and sensitivity, which is achieved by narrow chromatographic peaks and selective MS/MS detection. They allow separation and quantification of a large number of structurally similar oxylipins including positional isomeric (di-) hydroxy-fatty acids (-FA). RP-based methods with achiral stationary phases do not enable the separation of oxylipin enantiomers. However, this is key for understanding the formation routes and biology of these compounds as the stereochemistry directs biological activity, receptor interactions, and metabolic fate [8-10].

Numerous chromatographic methods for enantioselective oxylipin analysis are reported [10-15]. However, most of these methods cover only few oxylipins, except for a recent supercritical fluid chromatography- (SFC-) MS approach, which enables quantification of a wide range of octadecanoids [16]. Most commonly, amylose-based tris(3,5-dimethyl-phenylcarbamate) phases are employed for the separation of stereoisomeric oxylipins [10-12, 16-20]. Under RP conditions, this material exhibits suitable stereo selectivity, yielding adequate retention as well as separation of stereoisomeric oxylipins such as hydroxy-FA enantiomers [10-12, 21]. The chemical selectivity of this material towards positionally isomeric oxylipins is limited, which leads to their poor chromatographic resolution compared to RP chromatography [12, 20]. Given that isobaric oxylipins such as epoxy- and hydroxy-FA show similar fragment spectra and share mass transitions, chiral chromatography shows insufficient specificity for structural isomers [10]. Moreover, enantioselective chromatographic separation yields wider peaks compared to RP-(ultra-high performance) LC and thus lower sensitivity. As a result, the application of chiral chromatography for the comprehensive and quantitative analysis of oxylipins in biological samples is limited, and RP chromatography is the technique of choice for targeted oxylipin metabolomics [22].

Combining efficient RP chromatography and enantioselective separation is a promising approach for the sensitive and selective but stereospecific analysis of oxylipins. This is possible by heart-cutting two-dimensional (2D) chromatography. Heart-cutting enables the transfer of selected sections or peaks of the 1D chromatogram to a second column with orthogonal selectivity for further chromatographic separation. Achiral-chiral heart-cutting 2D-LC is frequently used for the analysis of amino acids [23, 24] or pharmaceuticals [25, 26]. By loop-based *multiple* cutting, the collection of a large number of 1D sections and subsequent 2D analysis is possible [27]. Despite its great potential, this has hardly been exploited for comprehensive targeted metabolomics.

In this work, an LC-MS/MS method has been developed which enables a specific and enantioselective quantitative analysis of oxylipins. An efficient RP LC-MS/MS separation was coupled with chiral

chromatography in a 2D multiple heart-cutting (MHC) setup. Due to the efficient RP separation in the first dimension, positionally isomeric oxylipins and isobaric compounds are separated. Heart-cutting of the entire 1D peak and efficient enantioselective separation by full-gradient elution on a chiral stationary phase enables sensitive and selective determination of a large number of oxylipin isomers, i.e. ARA-, EPA-, DHA-, linoleic-, and linolenic acid-derived hydroxy- and dihydroxy-FA.

The method described here is one of the most comprehensive multiple heart-cutting applications reported so far, and the first one for the analysis of oxylipins. This novel approach enables the elucidation of the formation pathways of oxylipins in biological samples based on quantitative oxylipin data and the ratio of the enantiomers with the same sensitivity and specificity of 1D RP-LC-MS/MS.

Experimental Section

Instrumental analytical methods

Chromatographic separation was carried out with an Agilent 1290 Infinity II system (Agilent Technologies, Waldbronn, Germany). In the 1D setup, the system comprises an autosampler, a binary pump, and a column oven. An established method for the analysis of more than 150 oxylipins was used in the first dimension [3]. Solvent A is a mixture of water and solvent B (95/5) with 0.1% acetic acid and solvent B consists of acetonitrile, methanol, and acetic acid (800/150/1). The oxylipins are separated on a C18 reversed-phase column (Zorbax Eclipse Plus C18, 2.1×150 mm, particle size 1.8 µm, pore size 9.5 nm, Agilent Technologies) at 40 °C with a flow rate of 0.3 mL/min and the following gradient: 21% B at 0 min, 21% B at 1.0 min, 26% B at 1.5 min, 51% B at 10 min, 66% B at 19 min, 98% B at 25.1 min, 98% B at 27.6 min, 21% B at 27.7 min, and 21% B at 31.5 min [3, 28]. For detection, the LC was coupled to a Sciex 6500+ QTrap triple quadrupole mass spectrometer (AB Sciex, Darmstadt, Germany) operated in negative electrospray ionization (ESI(-)) mode. In quantitative 1D analysis, the instrument was operated in scheduled multiple reaction monitoring (MRM), with a ±22 sec windows around the expected retention time and a cycle time of 0.4 min. The ion source settings were as follows: ionspray voltage: -4500 V, nebulizer gas (gas 1, zero air): 60 psi, drying gas (gas 2, zero air): 60 psi, temperature: 475 °C, curtain gas (N₂): 35 psi. The collision gas (N₂) was set to 12 psi. The injection volume was 5 µL. The 1D-LC and the MS were controlled using Analyst 1.7.3 Software (AB Sciex).

In the 2D setup, an additional binary pump and an additional oven as well as a 2D heart-cutting valve with active solvent modulation (ASM, 1.9 µL ASM capillary, ASM factor 3) and two multiple heart-cutting decks with six 40 µL sample loops each were integrated into to system (Fig. 1). All heart-cuts were triggered time-dependent based on the retention time of the oxylipins in the first dimension, which was determined prior to each 2D-LC batch (further details are described in the Supporting Information). 2D separation of the heart-cuts was carried out at 35 °C on a short 50×3.0 mm Chiralpak IA-U column, i.e. amylose tris(3,5-dimethylphenylcarbamate) material immobilized on 1.6 µm silica (Daicel, Osaka, Japan). Water with 10% acetonitrile and 0.1% acetic acid was used as solvent A and acetonitrile with 10% water and 0.1% acetic acid as solvent B. A flow of 0.9 mL/min was applied (backpressure 300–400 bar). The 2D gradient started with 5% B, which was kept for the duration of the ASM (0.14 min), then it was increased to 45% B in 0.01 min. From 0.15 min to 1.40 min the composition changed linear to 70% B, which was held for 0.3 min and subsequently, within 0.01 min, the initial conditions were

restored and held for 0.09 min, yielding a ²D cycle time of 1.80 min. An idle flow rate of 0.4 mL/min was used before and between the individual ²D runs. Mass spectrometric detection was carried out in negative MRM, with a dwell time of 12 ms for each transition. The following parameters of the ion source were adapted to the higher solvent flow: gas 2: 70 psi, temperature: 600 °C, curtain gas: 40 psi. The 2D-LC system was controlled using OpenLab CDS ChemStation Edition (C.01.10.) software (Agilent), while the mass spectrometer was controlled using Analyst 1.7.3 Software (AB Sciex).

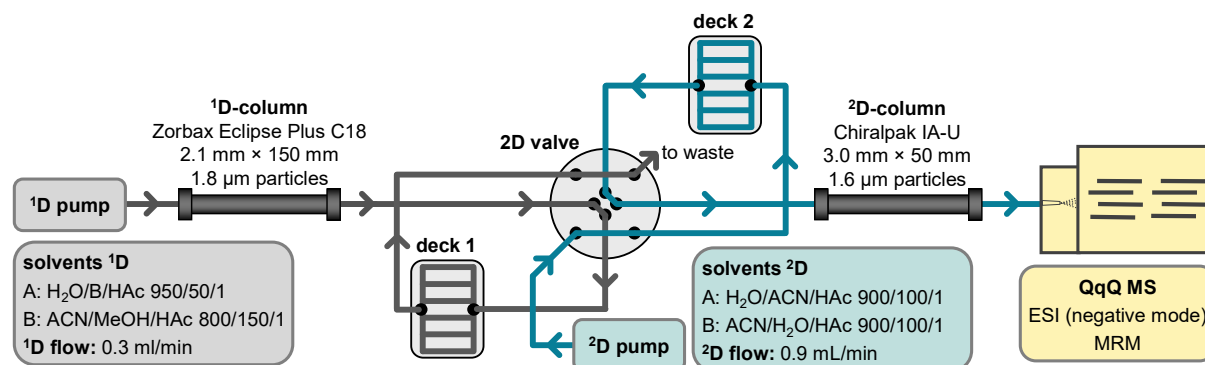


Figure 1. Setup of the multiple heart-cutting 2D-LC system. Gradient separation in the first dimension is carried out on an C18 stationary phase. The 2D valve directs the eluate of the first dimension to the parking decks. Each deck hosts six capillaries with a volume of 40 μ L which serve as sample loop for the ²D analysis. Gradient chiral separation in the second dimension is carried out on an amylose-based tris(3,5-dimethyl-phenylcarbamate) phase in reversed-phase mode. The oxylipins are detected by MS/MS.

Cell culture, enzymatic reactions and oxylipin extraction

2×10^6 HCA-7 cells were cultivated in 60 cm² dishes for 24 h [29]. *Tert*-butyl hydroperoxide (*t*BuOOH) or COX-inhibitors were added into the medium, and after 3 h (*t*BuOOH) or 24 h (COX-inhibitors) the cells were harvested using trypsin and sonicated in a mixture of water and methanol (50/50) containing an antioxidant solution [30]. M2-like primary human macrophages were generated and cultivated as previously described [3, 31]. For 15-LOX-catalyzed conversion of 5(*R,S*)-HETE, 5(*R,S*)-HEPE and 4(*R,S*)-HDHA 5 μ M of the compounds were incubated for 15 min with a homogenate of stably transfected HEK293T cells inducibly expressing *ALOX15* [30]. Enantioselective depletion of one stereoisomer from a racemic mixture was performed by Amano-Lipase PS catalyzed transesterification [32] Autoxidation of human plasma was induced by storing plasma in a non-light-protected environment at 20–23 °C for up to four days. The extraction of non-esterified oxylipins from plasma, serum, and cell homogenates was carried out by solid phase extraction on a non-polar C8/strong anion exchange mixed-mode material (Bond Elut Certify II, 200 mg, Agilent Technologies) as described [28, 33]. Details on the origin of the used chemicals and biological materials are described in the supporting information.

Results and Discussion

In order to enable both, sensitive and selective quantification of oxylipins and specific determination of enantiomeric ratios, we developed the first 2D targeted oxylipin metabolomics platform: By multiple heart-cutting (MHC), the oxylipins are collected from the first (RP) dimension and injected into the second dimension where chiral separation is performed (Fig 1). By separating and isolating isobaric

compounds and positional isomers in the first (RP) dimension, interferences in the chiral separation are minimized.

Quantitative 1D oxylipin metabolomics

The 1D setup is based on a well-established targeted LC-MS/MS lipidomics method covering 239 oxylipins. Quantification of oxylipins is performed by an external calibration using authentic reference standards with 29 isotopically labeled oxylipins as internal standards (Tab. S2-3) [3, 34]. With this method, hydroxy- and vicinal dihydroxy-FA elute as narrow peaks with full peak widths at half height (FWHM) of 4–5 sec over a broad window from 13 min to 22 min, ensuring an efficient chromatographic separation (Tab. 1) [3, 28, 33, 34]. This is crucial, because several critical separation pairs, i.e. isobaric compounds giving rise to similar fragment spectra, need to be chromatographically separated prior to MS/MS detection. Well-known examples of such pairs are hydroxy-FA and their corresponding epoxy derivatives (e.g. 15-HETE and 14(15)-EpETrE) [10]. However, this is also the case for several hydroxy-FA: For example, 7-HDHA shows a signal on the transition of 17-HDHA, 9- and 11-HEPE share characteristic fragments, as well as 9-HETE with 11-HETE and 12-HETE (Fig. S1).

Enantioselective 2D analysis of oxylipins

Chiral separation of oxylipins was carried out on a short (50 mm) column with < 2 μm particles. The amylose-based tris(3,5-dimethyl-phenylcarbamate) material yields good selectivity and allows the application of reversed-phase conditions. Active solvent modulation was used during the transfer of the heart-cuts to the 2D column, because this improved retention and separation of the enantiomers (Supporting Information). Due to the short column, a rapid (1.80 min total 2D run time) linear gradient of water and acetonitrile with 0.1% acetic acid could be used, which led to efficient separation of enantiomers of hydroxy- and vicinal dihydroxy-FA (Tab. 1, Tab. S5). An addition of methanol or *iso*-propanol to the solvents did not improve the separation (Tab. S4), although earlier reports showed clear changes in the selectivity for the separation of hydroxy-FA when different alcohols are used with the same stationary phase under normal-phase conditions [18, 35].

For the 2D interface, sample loops for the MHC with a volume of 40 μL (0.13 min of the 1D) were chosen. This corresponds to the 0.12 – 0.14 min of the 1D gradient and the full width at 10% peak height (FWTM) of the 1D peaks. The FWTM interval equals more than 96% of a Gaussian peak. Thus, practically the whole 1D peak is transferred to the second dimension without losing relevant amounts of the eluting oxylipin (Fig. 2A). At the same time, the transfer window is equally narrow as of the 1D peaks, preserving the separation and thus specificity of the first dimension.

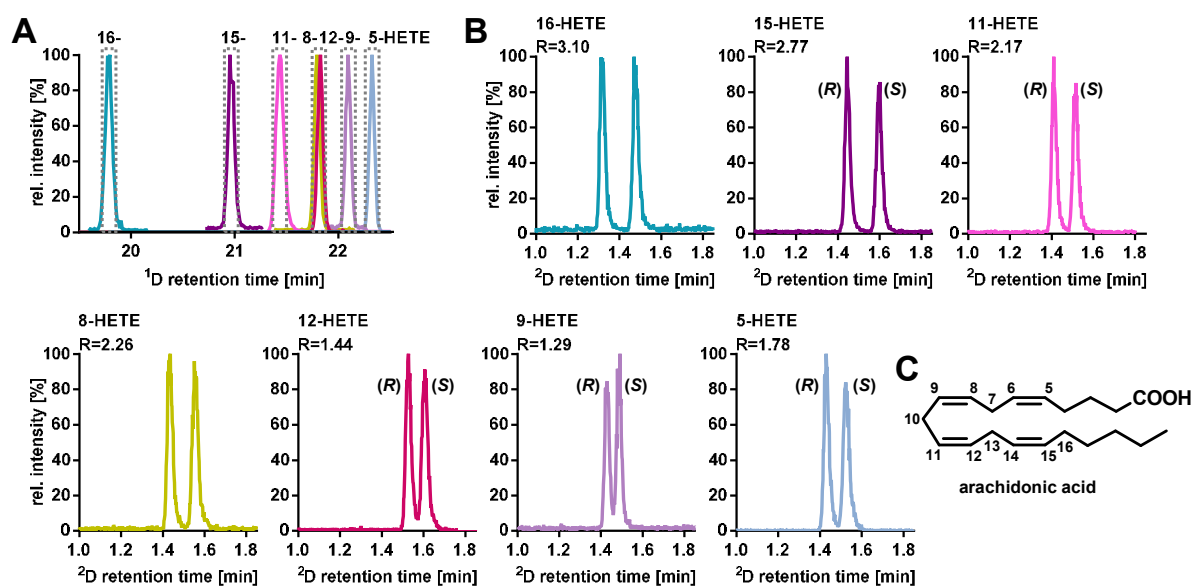


Figure 2. Chiral separation of arachidonic acid-derived oxylipins by means of 2D-LC-MS/MS. **A** ^1D chromatogram using a RP18 stationary phase (2.1 mm \times 150 mm, 1.8 μm particles) and acidified water and acetonitrile with methanol as solvents. Dashed lines indicate the volume which is collected in the ^2D sample loop. **B** Multiple heart-cut ^2D chromatograms following chiral separation using an amylose-based tris(3,5-dimethyl-phenylcarbamate) phase (3.0 mm \times 50 mm, < 2 μm particles) and acidified water and acetonitrile as eluents. Detection in both, 1D- and 2D-LC was carried by a triple quadrupole MS in MRM following ionization by electrospray ionization in negative mode. The separation of a racemic multi analyte oxylipin standard (50 nM) is shown. **C** Chemical structure of arachidonic acid with atom numbering indicating the positions of the hydroxy groups.

Heart-cutting can be triggered at any point in time, and thus it is possible to transfer every peak from the first dimension into the ^2D sample loop and subsequently further resolve it with the orthogonal selectivity in the second dimension. Thus, practically, the number of oxylipins that can be chirally separated in the second dimension in an individual analysis run is limited by the number of available loops of the 2D decks. Due to the rapid ^2D gradient (1.80 min) and the “smart peak parking” feature of the 2D-LC software, 12 to 15 heart-cuts can be collected within the runtime of the first dimension (32 min) resulting in total runtime of 32–45 min. Due to co-elution of non-isobaric compounds (Tab. 1) this allows the chiral analysis of up to 20 oxylipins (An exemplary sampling table is provided in the Supporting Information, Tab. S1). This is in our hands sufficient to address biological questions. Consistently, previous chiral methods used in the past cover a similar number of oxylipins, e.g. 16 pairs of enantiomers [10], a total of 37 lipid mediators [11] or 19 enantiomeric pairs along with two diastereomeric compounds [12]. However, if the enantiomeric fraction of all 45 oxylipins covered by the method should be analyzed at least two injections are necessary.

With 1.80 min, the duration of the ^2D gradient of this method is shorter in comparison to other MHC-applications, where ^2D chromatography with gradient elution is carried out in 5 min for the characterization of synthetic oligonucleotides [36], in 2.0 min for determining additives in polystyrene [27] or within 9 min for the analysis pyrrolizidine alkaloids in plants [37]. For enantioselective separation of amino acids, a considerably faster ^2D separation of 68 sec is described [24]. However, an isocratic separation was used here. This is common for achiral-chiral (multiple) heart-cutting methods, but not applicable for the structurally diverse class of oxylipins. Other 2D methods with a chiral second dimension aim to analyze individual heart-cuts, so that ^2D runtimes from four [23], six [25], or seven

minutes [26] up to more than 30 min [38] are used, which is not applicable for multiple heart-cutting methods.

The efficient chromatography in the second dimension yields full peak widths at half height (FWHM) < 2.5 sec for most of the oxylipin isomers (Tab. 1). This is in line with other chiral MHC 2D approaches, e.g. for the analysis of amino acids (FWHM ~2–4 sec) [24], and slightly narrower in comparison to a chiral 1D method in which the same < 2 μ m packing is used as enantioselective stationary phase for the separation of oxylipins (FWHM ~3 sec) [12]. However, in all other methods describing enantioselective analysis of oxylipins, considerably wider peaks (FWHM ~9 sec) are reported [10, 11].

With the rapid generic 2D gradient, the separation of 29 enantiomeric hydroxy-FA is achieved (Tab. 1): Seven ARA-derived hydroxy-FA enantiomers (HETE) are baseline separated (Fig. 2). Furthermore, ten pairs of stereo isomeric DHA- and seven EPA-derived hydroxy-FA (HDHA and HEPE, respectively) can be separated, as well as five hydroxy-octadecanoids from linolenic and linolenic acid (Tab. 1, Fig. S4). Of note, the developed method also includes the chiral analysis of 16 vicinal *threo*-dihydroxy-FA (Supporting Information). With this performance, separating > 40 pairs of oxylipin enantiomers, the described MHC-2D-method is the most comprehensive platform for the enantioselective analysis of oxylipins so far: There are established methods covering specific sets of oxylipins, e.g. ARA-derived hydroxy-FA [13, 19, 20] or the major oxidation products of ARA, EPA and DHA of the LOX- and COX-branch of the ARA-cascade [11, 39]. With few methods a comprehensive set of HETE-isomers, selected HEPE and HDHA together with PGE- and PGD-species [12] or with epoxy-FA [10] is analyzed. However, none of these methods provides a comparable comprehensive insight into the arachidonic acid cascade allowing a quantitative analysis together with the determination of the enantiomer ratio as the MHC-2D-LC-MS/MS platform presented here.

Determination of enantiomeric fractions

With the developed platform, quantitative analysis of oxylipins is extended by another important yet rarely addressed parameter: the ratio of enantiomers, expressed as enantiomeric fraction (EF), i.e. the proportion of one enantiomer in the sum of all ($EF = \frac{\text{peak area 1}}{\text{peak area 1} + \text{peak area 2}}$), which is slightly different to the earlier used enantiomeric excess ($ee = \frac{\text{peak area 1} - \text{peak area 2}}{\text{peak area 1} + \text{peak area 2}}$) [40]. Quantitative analysis and determination of EF are carried out in two individual runs. Quantification by 1D chiral methods is complicated because of the limited availability of corresponding isomerically pure standards, and the even more limited availability of deuterated analogs. The determination of the EF in the heart-cut by chiral separation in the second dimension does not require enantiomerically pure and isotope-labeled standards: The enantiomeric ratio can be directly calculated from the MRM peak area ratio of the enantiomers. Neither the extraction of oxylipins from biological samples [34, 41] nor the RP chromatography or heart-cutting and transfer discriminate one of the enantiomers. They show the exact same MS/MS behavior and as the solvent composition of the two peaks differs in the gradient by less than 10%, ionization efficiency is not affected [42]. Also, ion suppression is unlikely, because on the one hand, the interfering matrix is strongly reduced by the SPE-based sample preparation [43] and on the other hand only a small fraction of the 1D run is transferred to the second dimension. Thus, these

systematic method errors do not influence the determined EF. Most importantly, unlike previously available enantioselective one-dimensional methods for oxylipins, there is no risk of interference from isobaric molecules. These are either chromatographically separated in the first dimension or can be selectively detected without interference by specific mass transitions. Thus, following absolute quantification of the oxylipin by means of 1D RP-LC/MS, the ratio of the enantiomers can be determined reliably and precisely by MHC-2D-LC-MS/MS.

Even for only partially resolved isomers the enantiomeric ratio can be quantified even at a high enantiomeric excess, e.g. for 18(*R*)-HEPE and 18(*S*)-HEPE ($R=0.85$, Fig. 3A). If the concentration of both enantiomers is above the quantification limit, the EF can reliably be determined up to a ratio of 10%:90%.

Due to the narrow peaks in both dimensions and the optimized loop size for the heart-cut, the entire 1D peak is transferred to the second dimension. As a result, in the 2D enantioselective method, a sensitivity comparable to the high sensitivity of the 1D quantitative targeted metabolomics method is accomplished: For example, defining peaks with a signal-to-noise ratio ($S/N \geq 3$) as the limit of detection, 0.80 pg of 18-HEPE can be detected by means of 1D LC-MS/MS. The same S/N is achieved following MHC-2D-LC-MS/MS of 0.80 pg of each 18-HEPE enantiomer (Fig. 3B). For quantitative analyses, the lower limit of quantification (LLOQ) is defined by a $S/N \geq 5$ and an accuracy of $100 \pm 20\%$ within the calibration curve [44]. This value is typically 1.5-2.5 times higher than the LOD. Also with respect to the LOQ the performance of the one-dimensional method comparable to the two-dimensional method (Fig. S3). With this, the 2D method is more or equally sensitive as other less comprehensive enantioselective methods for the determination of oxylipins [10-13].

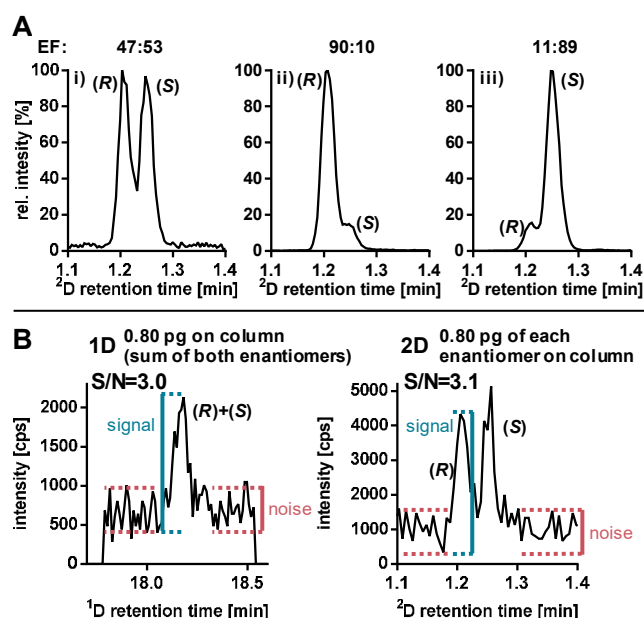


Figure 3. Determination of the enantiomeric fraction (EF) and detection limit of non-baseline separated 18-HEPE. **A** 2D chromatograms of (i) a racemic mixture of 18-HEPE, (ii) 18-(*R*)-HEPE along with a small amount of 18-(*S*)-HEPE and (iii) 18-(*R*)-HEPE with a large excess of 18-(*S*)-HEPE. **B** LC-ESI(-)-MS/MS chromatogram of an injection of a 0.5 nM racemic 18-HEPE standard (0.80 pg on column) measured by 1D-RP-LC-MS/MS and 2D chromatogram following heart-cutting and chiral separation of an 1 nM racemic 18-HEPE standard (1.6 pg total, i.e. 0.80 pg of each enantiomer on column). In the chromatograms the determination of the signal-to-noise ratio (S/N) is illustrated, showing the ($S/N \geq 3$) defined as limit of detection.

In order to evaluate the precision of the developed methodology, oxylipin concentrations and their EF were determined in three different sample types (i.e. human plasma, human serum and oxidized human

plasma with exceptionally high levels of oxylipins) on three different days. The high precision (< 15% relative standard deviation (RSD)) of quantitative oxylipin analysis in plasma and serum within and across different batches (Tab. S6) fulfills criteria of international guidelines [44] and is comparable or better than other targeted oxylipin methods [11, 12, 28, 33]. The determination of the EF by MHC-2D-LC-MS/MS yields even more precise results: RSD of less than $\leq 5\%$ in the inter-day comparison were observed, and except few oxylipins on individual days, the method yields high intra-day precision with an RSD < 10% (Tab. S6).

In oxidized plasma with artificially high oxylipin levels, the EF of hydroxy-FA (50%:50%) indicates racemic mixtures, underlining the autoxidative origin of these oxylipins (Tab. S6). Only for the vicinal dihydroxy-FA 14,15-DiHETrE a clear excess of one enantiomer was found (EF 16%:84%). Along with the at least ten times lower concentration of this oxylipin compared to others in the oxidized plasma, enzymatic formation can be assumed. 14,15-DiHETrE is formed by (soluble) epoxide hydrolases and its precursor 14(15)-EpETrE by CYP [45] and is not affected by autoxidation and blood coagulation. Consistently, similar concentrations as well as EF were found in non-oxidized plasma as well as serum. In well-prepared and stored plasma, the concentrations of hydroxy-FA are lower than in the oxidized one, and those oxylipins which are canonical products of human lipoxygenases, e.g. 5-HETE, 12-HETE and 15-HETE, show an excess of one enantiomer (EF > 60%) (Tab. S6). Consistent with the activation of platelets, 12-HETE, a downstream product of platelet-derived 12-LOX [46], is dramatically (~150 fold) increased in serum compared to plasma, with a massive excess of 12(S)-HETE (EF: 99.7%) (Tab. S6).

Enantioselective analysis of oxylipins in human cells

The autoxidation of fatty acids is stereorandom, giving equally rise to both, (*R*)- and (*S*)-enantiomers of hydro(pero)xy-FA [47]. On the contrary, enzymatically catalyzed formation of hydroxy-FA is stereo specific, for example human lipoxygenases such as platelet-derived 12-LOX give rise to (*S*)-hydro(pero)xy-FA (Tab. S6) [46]. Thus, the EF can be used to differentiate the formation route of oxylipins. This was demonstrated by applying the developed MHC-2D-LC-MS/MS method on the analysis of hydroxy-FA and their modulation in HCA-7 cells. This human colon carcinoma cell line overexpresses *PTGS2*, the cyclooxygenase-2 (COX-2)-coding gene, yielding a high abundance and activity of the COX-2 [48]. Treatment of this cell line with the irreversible COX inhibitor acetylsalicylic acid (ASA) or the non-competitive selective COX-2 inhibitor celecoxib decreased the concentration of oxylipins resulting from COX-2 activity, such as PGE₂ and 12-HHTrE (Fig. S5) and the side product 11-HETE (Fig. 4A). Chiral analysis revealed predominant formation of 11(*R*)-HETE, and the stereoisomerism was not affected by ASA or celecoxib (Fig. 4A, Fig. 4D). Incubation with celecoxib also reduced 15-HETE levels in the cells without effecting the EF. However, following ASA treatment of HCA-7 cells, an increased 15-HETE formation was observed (Fig. 4B). While non-treated as well as celecoxib-treated cells showed an excess of 15(*S*)-HETE (EF: 80%), ASA incubation yields almost enantiopure formation of 15(*R*)-HETE (EF: 92%) (Fig. 4B, Fig. 4E). These findings are consistent with the reported peroxidase activity of COX, by which 11(*R*)-H(p)ETE and 15(*S*)-H(p)ETE are formed as side products [49], and with the finding that inhibition with ASA leads to an increase in 15-HETE formation [50]. Mechanistically, the inhibition of COX-2 by ASA results from acetylation of Ser-530 in the

active site of the enzyme. However, this modification of the enzyme does not inhibit the COX-2-catalyzed formation of 15-HETE, but changes the stereospecificity of the reaction towards 15(*R*)-HETE [51]. Based on that, the formation of several specific “aspirin” triggered oxylipins explaining part of ASA’s pharmacological effects have been described [52].

5-HETE is detected in HCA-7 cells only at low levels and with an almost racemic mixture of the enantiomers (Fig. 4C, Fig. 4F), indicating non-enzymatic formation. This is in line with the absence of 5-LOX in this colon cell line, which is only expressed in immune cells [52]. 5-HETE levels increase following treatment with the oxidative stress-causing agent *tert*-butyl hydroxide (*t*BuOOH) (Fig 4C). The EF of 5(*R*)- and 5(*S*)-HETE does not change following *t*BuOOH treatment, as this agent induces non-enzymatic lipid (per-)oxidation (Fig. 4C, Fig. 4F).

This application shows that the developed platform provides sound quantitative data on oxylipin levels in biological samples on the one hand and reliable data on the enantiomeric ratios on the other, giving insights in the formation pathways of oxylipins and their modulation.

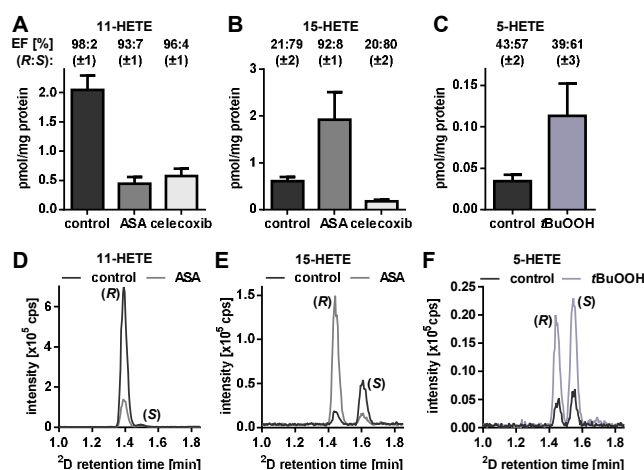


Figure 4. Enzymatic and non-enzymatic formation of hydroxy-fatty acids in cell culture. COX-2 expressing HCA-7 cells were incubated with 100 μ M acetylsalicylic acid (ASA) for 24 h, 10 μ M celecoxib for 24 h or 100 μ M *tert*-butyl hydroperoxide (*t*BuOOH) for 3 h. **A** Inhibition of COX-2-catalyzed 11-HETE formation by ASA and celecoxib. **B** Inhibition of COX-2-catalyzed 15-HETE formation by celecoxib and 15(*R*)-HETE formation by acetylated COX-2. **C** *tert*-Butyl hydroperoxide-induced increase of 5-HETE concentrations. **D** 2 D-MRM chromatogram of 11-HETE, indicating COX-2-catalyzed formation of 11(*R*)-HETE, which is inhibited by ASA. **E** 2 D-MRM chromatogram of 15-HETE, indicating the increased formation of 15(*R*)-HETE by ASA acetylated COX-2. **F** 2 D-MRM chromatogram of 5-HETE indicating racemic formation of 5(*R,S*)-HETE by non-enzymatic oxidation which is induced by *t*BuOOH.

Analysis of dihydroxy-fatty acids in primary human macrophages and human plasma

Multiple-hydroxy fatty acids – several are referred to as specialized pro-resolving mediators (SPM) – are discussed to exhibit potent physiological effects in the regulation of inflammatory processes. However, the signaling, occurrence and formation routes of these compounds are largely unclear.[52] While trihydroxy-fatty acids are not reliably detected in biological samples[52] such as leucocytes,[53] dihydroxy-fatty acids are consistently reported in macrophages.[53] However, these compounds could be formed by autoxidation as well as via the enzymatic pathways suggested for SPM formation.

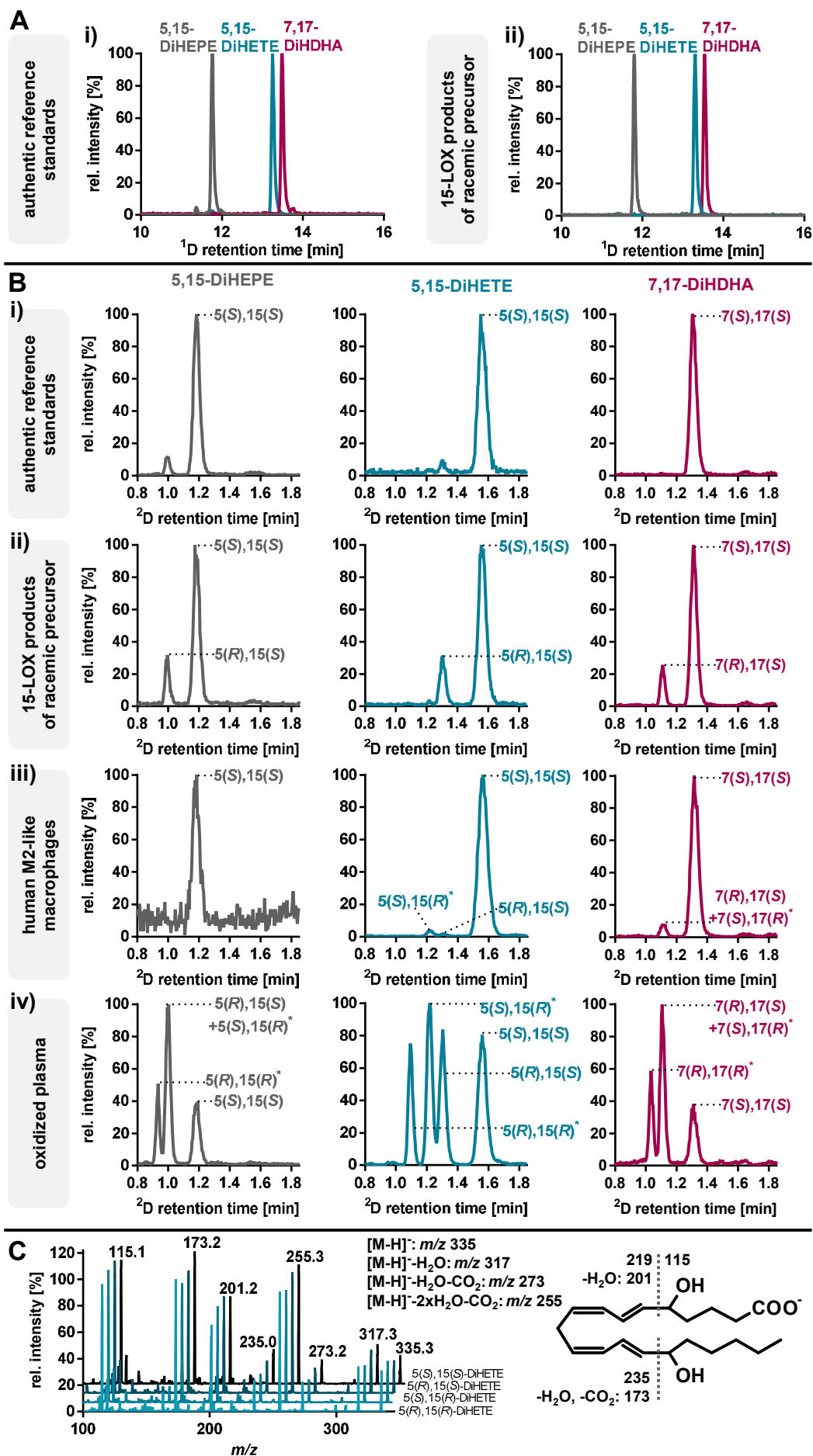


Figure 5. Separation of dihydroxy ARA, EPA and DHA by enantioselective heart-cutting 2D-LC. **A** RP chromatograms (MRM signals) of (i) a standard mixture (50 nM) containing 5(*S*),15(*S*)-DiHETE, 5(*S*),15(*S*)-DiHEPE and 7(*S*),17(*S*)-DiHDHA and (ii) a mixture of 5(*R/S*),15(*S*)-DiHETE, 5(*R/S*),15(*S*)-DiHEPE and 7(*R/S*),17(*S*)-DiHDHA, which was generated by conversion of 5(*R,S*)-HETE, 5(*R,S*)-HEPE and 7(*R,S*)-HDHA by human 15-LOX. **B** ²D chromatograms (MRM signals) following chiral separation of (i) 5,15-DiHETE, 5,15-DiHEPE and 7,17-DiHDHA derived from reference standards, (ii) enzymatically formed diastereomers, (iii) human M2-like macrophages and (iv) oxidized (commercial) human plasma. **C** Exemplary identical MS² spectra of the four stereoisomers of 5,15-DiHETE from oxidized human plasma. The following MRM transitions were used: 5,15-DiHETE: *m/z* 335>173; 5,15-DiHEPE: *m/z* 333>173; 7,17-DiHDHA: *m/z* 359>141. *: Stereo configuration of these isomers is estimated based on elution order.

In order to investigate the formation route of these dihydroxy-fatty acids, the MHC-2D-LC-MS/MS-method was applied. As expected, the enantiopure synthetic standards of 5(*S*),15(*S*)-DiHETE, 5(*S*),15(*S*)-DiHEPE (resolvin E4) as well as 7(*S*),17(*S*)-DiHDHA (resolvin D5) showed only one peak in both, ¹D- (Fig. 5A) and ²D (Fig. 5B) chromatograms. By enantioselective conversion of racemic 5-HETE, 5-HEPE and 7-HDHA by human 15-LOX (only giving rise to (*S*)-hydro(pero)xy-FA [54]) the diastereomeric pairs 5(*R*),15(*S*)- and 5(*S*),15(*S*)-DiHETE, 5(*R*),15(*S*)- and 5(*S*),15(*S*)-DiHEPE as well as 7(*R*),17(*S*)- and 7(*S*),17(*S*)-DiHDHA were generated. Chromatographic separation of these diastereomers was not possible by 1D RP chromatography (Fig. 5A). Coelution of these diastereomers was also found on other RP materials (Fig. S6), despite several diastereomeric oxylipins can be effectively separated by RP chromatography, for example, 7(*R*),14(*S*)- and 7(*S*),14(*S*)-dihydroxy-4(*Z*),8(*E*),10(*E*),12(*Z*),16(*Z*),19(*Z*)-DHA, (maresin 1 and 7(*S*)-maresin 1) [33], as well as 10(*S*),17(*S*)-dihydroxy-4(*Z*),7(*Z*),11(*E*),13(*Z*),15(*E*),19(*Z*)-docosahexaenoic acid (protectin DX) and its 10(*R*),17(*S*)-diastereomer (Fig. S8).

Following heart-cutting and chromatography with a chiral stationary phase, baseline separation of all diastereomers was achieved and stereo information could be assigned by comparison with the enantiopure reference standard (Fig. 5B).

When analyzing human M2-like macrophages, which were derived from human monocytes by differentiation with colony-stimulating factor- (CSF-) 1 and interleukin- (IL-) 4, in which 15-LOX is highly abundant [3], dominant amounts of 5(*S*),15(*S*)-DiHETE, 5(*S*),15(*S*)-DiHEPE and 7(*S*),17(*S*)-DiHDHA were found. The (*R,R*)-enantiomers were not detected, and only negligible amounts of the respective diastereomers were present (Fig. 5B). This demonstrates that these dihydroxy-fatty acids which are present in quantities of 20-50 pmol per mg protein in the macrophages, are of enzymatic origin. The fact that only the (*S,S*) enantiomer is detected supports the assumption of their formation by consecutive LOX-catalyzed reactions [52, 53]. Accordingly, of the analogous compound 10,17-DiHDHA two stereoisomers, i.e. 10(*S*),17(*S*)-DiHDHA ("protectin DX") and 10(*R*),17(*S*)-DiHDHA, are detected in macrophages, since only the oxidation at position 17 is enzymatically catalyzed (by 15-LOX), while the one at position 10 is not (Fig. S8). It is postulated that the 17(*S*)-hydroperoxy-DHA formed by 15-LOX can be converted to 10(*R*),17(*S*)-DiHDHA with an (*E,E,Z*)-configured triene system ("neuroprotection D1") [55]. ²D chiral analysis of the presumptive peak of "neuroprotection D1" revealed that the single peak detected following RP chromatography consists of at least three isomers of which "neuroprotection D1" is not the major component (Fig. S8). It can therefore be assumed that this oxylipin is not formed by controlled enzymatic reactions.

Few studies also report the occurrence of dihydroxy FA in (commercial) plasma or serum [56] and we found large amounts in commercial plasma (Fig. 5, Fig. S7). However, consistent with earlier reports

[52, 57], 5,15-DiHEPE, 5,15-DiHETE and 7,17-DiHDHA could not be detected in carefully collected and freshly prepared plasma from healthy human subjects (Fig. 6). Analyzing (inappropriately) stored plasma, which was kept at room temperature for few hours up to several days, a rapid increase and dihydroxy-FA is observed (Fig 6). This indicates that a major portion, if not all 5,15-DiHEPE, 5,15-DiHETE and 7,17-DiHDHA, reported in plasma is formed artificially by autoxidation during sample preparation or storage.

Chiral analysis following heart-cutting of 5,15-DiHETE from all oxidized plasmas yielded four peaks (Fig. 5B) showing the exactly same MS² spectra (Fig. 5C). Based on the identical retention times as the enzymatically generated standards, two peaks were identified as 5(*R*),15(*S*)- and 5(*S*),15(*S*)-DiHETE. The two other peaks were assigned to the corresponding enantiomers, assuming, based on the general earlier retention time of *R*-hydroxy-FA, that the (*R*),(*R*) isomer elutes first. Following ²D chiral analysis of 5,15-DiHEPE and 7,17-DiHDHA from oxidized plasma three peaks are detected, with one peak twice as high as the others (Fig. 5B). It can be assumed that two of the four stereoisomers are coeluting. Based on the retention time and peak height presumably 5(*R*),15(*S*)- and 5(*S*),15(*R*)-DiHEPE as well as 7(*R*),17(*S*)- and 7(*S*),17(*R*)-DiHDHA elute together (Fig. 5B). The stereoisomers resulting from the catalytic activity of 5-LOX and 15-LOX, i.e. bearing (*S,S*) configuration of the hydroxy-groups, is thus baseline-separated from its enantiomer and diastereomers. This allows to distinguish it from non-enzymatically formed oxidation products. The occurrence of all four stereo isomers in the plasma confirms the autoxidative origin of the dihydroxy-FA. Due to the suggested biological role of 5(*S*),15(*S*)-DiHEPE (resolvin E4) and 7(*S*),17(*S*)-DiHDHA (resolvin D5), a large number of studies report their occurrence in biological samples [52], however their stereo configuration is rarely addressed. However, we demonstrate here, that RP chromatography not only leads to the expected co-elution of their enantiomers but also of the diastereomers. Thus, if chromatography without a chiral selector is performed, all stereoisomers in sum are determined, and not one specific isomer of the lipid. Our data shows that, indeed, 5(*S*),15(*S*)-DiHEPE (resolvin E4) and 7(*S*),17(*S*)-DiHDHA (resolvin D5) are present in human M2-like macrophages. However, in other biological samples, all four isomers of the dihydroxy-FA can occur as demonstrated for oxidized plasma (Fig. 5B). Reporting 5,15-DiHEPE and 7,17-DiHDHA as resolvin E4 and resolvin D5, respectively, following RP chromatography is therefore misleading. Only chiral separation as developed here allows to demonstrate the presence of 5(*S*),15(*S*)-DiHEPE (resolvin E4) and 7(*S*),17(*S*)-DiHDHA (resolvin D5) in biological samples.

The developed MHC-2D-LC-MS/MS method is therefore an important tool for the separation of both, enantiomeric and stereoisomeric oxylipins. With that, the stereo configuration can be unveiled enabling a better characterization of the oxylipins found in biological samples and their formation route.

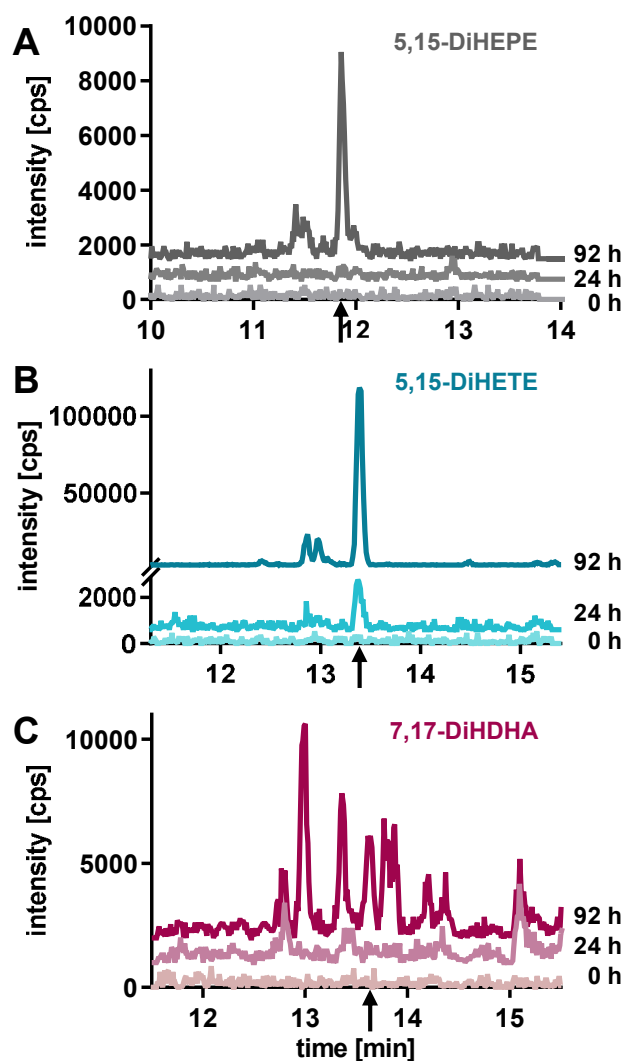


Figure 6. Formation of dihydroxy-EPA (A), ARA (B) and DHA (C) in human plasma during storage at room temperature. Human plasma was stored at room temperature for 1 – 4 days. Shown are the 1D RP chromatograms (MRM signals) at baseline (0 h) as well as after 24 h and 92 h. The arrows indicate the retention time of the indicated dihydroxy-FA. The following MRM transitions were used: 5,15-DiHETE: m/z 335>173; 5,15-DiHEPE: m/z 333>173; 7,17-DiHDHA: m/z 359>141. The signals after 24 h and 92 h of 5,15-DiHEPE and 7,17-DiHDHA are shown with an offset of 750 cps and 1000 cps, respectively. The 24 h signal of 5,15-DiHETE is shown with an offset of 600 cps, and the signal of the 92 h signal with an offset of 2800 cps. Chiral 2D analysis of the peaks of 15-DiHETE, 5,15-DiHEPE and 7,17-DiHDHA unveiled four (three) peaks as shown in Fig. 5B for oxidized plasma.

Conclusions

Comprehensive but selective and sensitive quantitative analysis of lipid mediators is key to elucidating their biological roles. In order to understand changes in the oxylipin pattern in (patho-) physiological conditions or by the use pharmaceutical drugs, however, the enantioselective analysis is urgently required. In the present study, a multiple heart-cutting achiral-chiral 2D-LC-MS/MS method was developed: Efficient 1D RP chromatography enables reliable separation of regioisomeric oxylipins and allows sensitive quantification of large number of these lipids in biological samples in sub-nanomolar concentrations. By multiple heart-cutting from this efficient RP separation and subsequent enantioselective separation on a chiral stationary phase, the challenge of interference from isobaric compounds is addressed, which hampers the application of 1D chiral methods. The rapid ²D full gradient separation allows the separation of an unprecedented number of isomer pairs of oxylipins within a ²D

cycle time of 1.80 min. The use of an optimal ²D samples loop size enables the transfer of the whole ¹D peaks, leading to the same sensitivity as in 1D methods. The developed method is the first combination of targeted oxylipin metabolomics and enantioselective analysis in two dimensional LC. This new dimension of oxylipin analysis can be readily used to extend existing LC-MS/MS oxylipin platforms. Clinical samples can be analyzed for enantiomeric ratios from the same sample without additional sample preparation steps or even additional sample materials. With these new possibilities the method paves the route to gain new insights into the pathways of oxylipin formation in biological samples leading to a better understanding of their role in physiological processes.

Supporting Information

Detailed description of instrumental methods and materials; Data about interferences in MRM-detection of oxylipins; Data about the impact of the mobile phase on enantioselective separation of oxylipins; Optimization of ASM settings; Figure showing the LLOQ (S/N>5) in the second dimension; Data about the chiral separation of vicinal dihydroxy-FA; Chromatograms of RP- and chiral separation of EPA, DHA, linoleic acid and linoleic acid-derived oxylipin isomers; Intra- and interday variability of determined oxylipin concentrations and isomeric fractions in human plasma and serum; Data about COX-2 inhibition in HCA7-cells; Lack of separation of dihydroxy-fatty acid diastereomers by reversed-phase chromatography; ¹D and ²D chromatograms of two MRM transitions for the detection of 5,15-DiHEPE and 7,17-DiHDPE, Enantioselective analysis of 10,17-DiHDHA isomers

CRedit authorship contribution statement

NK: Conceptualization, Methodology, Investigation, Validation, Formal analysis Writing - Original Draft, Writing - Review & Editing; AL: Investigation, Formal analysis, Writing - Review & Editing; RK: Investigation, Formal analysis, Writing - Review & Editing; NHS: Conceptualization, Methodology, Resources, Writing - Original Draft, Writing - Review & Editing, Funding acquisition

Acknowledgment

Our work is supported by grant (SCHE 1801) of the German Research Foundation to NHS and by a Ph.D. scholarship from the Friedrich-Ebert-Stiftung e.V. to RK.

list of abbreviations

¹ D, first dimension	DiHDPE, dihydroxydocosapentaenoic acid
² D, second dimension	DiHEPE, dihydroxyeicosapentaenoic acid
ARA, arachidonic acid	DiHETE, dihydroxyeicosatetraenoic acid
ASA, acetylsalicylic acid	DiHETrE, dihydroxyeicosatrienoic acid
ASM, active solvent modulation	DiHODE, dihydroxyoctadienoic acid
CYP, cytochrome P450 monooxygenase	DiHOME, dihydroxyoctadecenoic acid
COX, cyclooxygenase	EF, enantiomeric fraction
DHA, docosahexanoic acid	EPA, eicosapentaenoic acid
DiHDHA, dihydroxydocosahexanoic acid	FA, fatty acid

HDHA, hydroxydocosahexaenoic acid	LOX, lipoxygenase
HEPE, hydroxyeicosapentaenoic acid	MHC, multiple heart-cutting
HETE, hydroxyeicosatetraenoic acid	NP, normal phase
HODE, hydroxyoctadienoic acid	RP, reversed-phase
HOTrE, hydroxyoctatrienoic acid	<i>t</i> BuOOH, <i>tert</i> -butyl hydroperoxide
LC, liquid chromatography	

References

1. Gabbs, M., et al., *Advances in Our Understanding of Oxylipins Derived from Dietary PUFAs*. *Advances in Nutrition*, 2015. **6**(5): p. 513-540.
2. Buczynski, M.W., D.S. Dumlao, and E.A. Dennis, *Thematic Review Series: Proteomics. An integrated omics analysis of eicosanoid biology1[S]*. *Journal of Lipid Research*, 2009. **50**(6): p. 1015-1038.
3. Hartung, N.M., et al., *Development of a quantitative proteomics approach for cyclooxygenases and lipoxygenases in parallel to quantitative oxylipin analysis allowing the comprehensive investigation of the arachidonic acid cascade*. *Analytical and Bioanalytical Chemistry*, 2023. **415**(5): p. 913-933.
4. Dumlao, D.S., et al., *High-throughput lipidomic analysis of fatty acid derived eicosanoids and N-acyl ethanolamines*. *Biochimica et Biophysica Acta (BBA) - Molecular and Cell Biology of Lipids*, 2011. **1811**(11): p. 724-736.
5. Berkecz, R., M. LÍsa, and M. Holčápek, *Analysis of oxylipins in human plasma: Comparison of ultrahigh-performance liquid chromatography and ultrahigh-performance supercritical fluid chromatography coupled to mass spectrometry*. *Journal of Chromatography A*, 2017. **1511**: p. 107-121.
6. Chen, G.-y. and Q. Zhang, *Comprehensive analysis of oxylipins in human plasma using reversed-phase liquid chromatography-triple quadrupole mass spectrometry with heatmap-assisted selection of transitions*. *Analytical and Bioanalytical Chemistry*, 2019. **411**(2): p. 367-385.
7. Pedersen, T.L., I.J. Gray, and J.W. Newman, *Plasma and serum oxylipin, endocannabinoid, bile acid, steroid, fatty acid and nonsteroidal anti-inflammatory drug quantification in a 96-well plate format*. *Analytica Chimica Acta*, 2021. **1143**: p. 189-200.
8. Powell, W.S. and J. Rokach, *Biosynthesis, biological effects, and receptors of hydroxyeicosatetraenoic acids (HETEs) and oxoeicosatetraenoic acids (oxo-ETEs) derived from arachidonic acid*. *Biochimica et Biophysica Acta (BBA) - Molecular and Cell Biology of Lipids*, 2015. **1851**(4): p. 340-355.
9. Powell, W.S., F. Gravelle, and S. Gravel, *Metabolism of 5(S)-hydroxy-6,8,11,14-eicosatetraenoic acid and other 5(S)-hydroxyeicosanoids by a specific dehydrogenase in human polymorphonuclear leukocytes*. *Journal of Biological Chemistry*, 1992. **267**(27): p. 19233-19241.
10. Blum, M., et al., *Chiral lipidomics of monoepoxy and monohydroxy metabolites derived from long-chain polyunsaturated fatty acids[S]*. *Journal of Lipid Research*, 2019. **60**(1): p. 135-148.

11. Toewe, A., et al., *Simultaneous determination of PUFA-derived pro-resolving metabolites and pathway markers using chiral chromatography and tandem mass spectrometry*. *Analytica Chimica Acta*, 2018. **1031**: p. 185-194.
12. Cebo, M., et al., *Enantioselective ultra-high performance liquid chromatography-tandem mass spectrometry method based on sub-2 μ m particle polysaccharide column for chiral separation of oxylipins and its application for the analysis of autoxidized fatty acids and platelet releasates*. *Journal of Chromatography A*, 2020. **1624**: p. 461206.
13. Isse, F.A., et al., *The enantioselective separation and quantitation of the hydroxy-metabolites of arachidonic acid by liquid chromatography – tandem mass spectrometry*. *Prostaglandins & Other Lipid Mediators*, 2023. **165**: p. 106701.
14. Bayer, M., A. Mosandl, and D. Thaçi, *Improved enantioselective analysis of polyunsaturated hydroxy fatty acids in psoriatic skin scales using high-performance liquid chromatography*. *Journal of Chromatography B*, 2005. **819**(2): p. 323-328.
15. Schneider, C., et al., *Enantiomeric Separation of Hydroxy and Hydroperoxy Eicosanoids by Chiral Column Chromatography*, in *Methods in Enzymology*. 2007, Academic Press. p. 145-157.
16. Quaranta, A., et al., *Development of a Chiral Supercritical Fluid Chromatography–Tandem Mass Spectrometry and Reversed-Phase Liquid Chromatography–Tandem Mass Spectrometry Platform for the Quantitative Metabolic Profiling of Octadecanoid Oxylipins*. *Analytical Chemistry*, 2022. **94**(42): p. 14618-14626.
17. Serhan, C.N., et al., *Maresins: novel macrophage mediators with potent antiinflammatory and proresolving actions*. *Journal of Experimental Medicine*, 2008. **206**(1): p. 15-23.
18. Schneider, C., W.E. Boeglin, and A.R. Brash, *Enantiomeric Separation of Hydroxy Eicosanoids by Chiral Column Chromatography: Effect of the Alcohol Modifier*. *Analytical Biochemistry*, 2000. **287**(1): p. 186-189.
19. Mazaleuskaya, L.L., et al., *Analysis of HETEs in human whole blood by chiral UHPLC-ECAPCI/HRMS*. *Journal of Lipid Research*, 2018. **59**(3): p. 564-575.
20. Tacconelli, S., et al., *Pharmacological characterization of the biosynthesis of prostanoids and hydroxyeicosatetraenoic acids in human whole blood and platelets by targeted chiral lipidomics analysis*. *Biochimica et Biophysica Acta (BBA) - Molecular and Cell Biology of Lipids*, 2020. **1865**(12): p. 158804.
21. Fu, X., et al., *UHPLC-MS/MS method for chiral separation of 3-hydroxy fatty acids on amylose-based chiral stationary phase and its application for the enantioselective analysis in plasma and platelets*. *Journal of Pharmaceutical and Biomedical Analysis*, 2023. **223**: p. 115151.
22. Gladine, C., et al., *MS-based targeted metabolomics of eicosanoids and other oxylipins: Analytical and inter-individual variabilities*. *Free Radical Biology and Medicine*, 2019. **144**: p. 72-89.
23. Guillén-Casla, V., et al., *Direct chiral determination of free amino acid enantiomers by two-dimensional liquid chromatography: application to control transformations in E-beam irradiated foodstuffs*. *Analytical and Bioanalytical Chemistry*, 2010. **397**(1): p. 63-75.

24. Karongo, R., et al., *Enantioselective multiple heart cutting online two-dimensional liquid chromatography-mass spectrometry of all proteinogenic amino acids with second dimension chiral separations in one-minute time scales on a chiral tandem column*. *Analytica Chimica Acta*, 2021. **1180**: p. 338858.
25. Yang, Y., et al., *Chiral Determination of Salbutamol, Salmeterol and Atenolol by Two-Dimensional LC–LC: Application to Urine Samples*. *Chromatographia*, 2012. **75**(23): p. 1365-1375.
26. Peñín-Ibáñez, M., M.J. Santos-Delgado, and L.M. Polo-Diez, *Determination of profens in pharmaceuticals by heart-cut achiral-chiral two-dimensional HPLC*. *SEPARATION SCIENCE PLUS*, 2018. **1**(3): p. 168-176.
27. Pursch, M. and S. Buckenmaier, *Loop-Based Multiple Heart-Cutting Two-Dimensional Liquid Chromatography for Target Analysis in Complex Matrices*. *Analytical Chemistry*, 2015. **87**(10): p. 5310-5317.
28. Rund, K.M., et al., *Development of an LC-ESI(-)-MS/MS method for the simultaneous quantification of 35 isoprostanes and isofurans derived from the major n3- and n6-PUFAs*. *Analytica Chimica Acta*, 2018. **1037**: p. 63-74.
29. Willenberg, I., A.K. Meschede, and N.H. Schebb, *Determining cyclooxygenase-2 activity in three different test systems utilizing online-solid phase extraction-liquid chromatography-mass spectrometry for parallel quantification of prostaglandin E2, D2 and thromboxane B2*. *Journal of Chromatography A*, 2015. **1391**: p. 40-48.
30. Goebel, B., et al., *Development of a cell-based model system for the investigation of ferroptosis*. *Frontiers in Cell Death*, 2023. **2**.
31. Ebert, R., et al., *Long-term stimulation of toll-like receptor-2 and -4 upregulates 5-LO and 15-LO-2 expression thereby inducing a lipid mediator shift in human monocyte-derived macrophages*. *Biochimica et Biophysica Acta (BBA) - Molecular and Cell Biology of Lipids*, 2020. **1865**(9): p. 158702.
32. Jübermann, M., *Totalsynthese von 18-HEPE und unnatürlichen Hydroxy-PUFAs*. 2018, Bergische Universität Wuppertal: Wuppertal. p. 1 Online-Ressource (184 Blätter).
33. Kutzner, L., et al., *Development of an Optimized LC-MS Method for the Detection of Specialized Pro-Resolving Mediators in Biological Samples*. *Frontiers in Pharmacology*, 2019. **10**.
34. Koch, E., et al., *Stability of oxylipins during plasma generation and long-term storage*. *Talanta*, 2020. **217**: p. 121074.
35. Lee, S.H., et al., *Targeted lipidomics using electron capture atmospheric pressure chemical ionization mass spectrometry*. *Rapid Communications in Mass Spectrometry*, 2003. **17**(19): p. 2168-2176.
36. Li, F., et al., *Multiple heart-cutting mixed-mode chromatography-reversed-phase 2D-liquid chromatography method for separation and mass spectrometric characterization of synthetic oligonucleotides*. *Journal of Chromatography A*, 2020. **1625**: p. 461338.

37. van de Schans, M.G.M., et al., *Multiple heart-cutting two dimensional liquid chromatography quadrupole time-of-flight mass spectrometry of pyrrolizidine alkaloids*. Journal of Chromatography A, 2017. **1503**: p. 38-48.
38. Koga, R., et al., *Enantioselective two-dimensional high-performance liquid chromatographic determination of N-methyl-D-aspartic acid and its analogues in mammals and bivalves*. Journal of Chromatography A, 2012. **1269**: p. 255-261.
39. Oh, S.F., T.W. Vickery, and C.N. Serhan, *Chiral lipidomics of E-series resolvins: Aspirin and the biosynthesis of novel mediators*. Biochimica et Biophysica Acta (BBA) - Molecular and Cell Biology of Lipids, 2011. **1811**(11): p. 737-747.
40. Tiritan, M.E., et al., *Enantiomeric ratios: Why so many notations?* Journal of Chromatography A, 2018. **1569**: p. 1-7.
41. Ostermann, A.I., et al., *Targeting esterified oxylipins by LC-MS - Effect of sample preparation on oxylipin pattern*. Prostaglandins & Other Lipid Mediators, 2020. **146**: p. 106384.
42. Hartung, N.M., et al., *A strategy for validating concentrations of oxylipin standards for external calibration*. Prostaglandins & Other Lipid Mediators, 2019. **141**: p. 22-24.
43. Ostermann, A.I., I. Willenberg, and N.H. Schebb, *Comparison of sample preparation methods for the quantitative analysis of eicosanoids and other oxylipins in plasma by means of LC-MS/MS*. Analytical and Bioanalytical Chemistry, 2015. **407**(5): p. 1403-1414.
44. . European Medicines Agency: ICH guideline M10 on bioanalytical method validation and study sample analysis, EMA/CHMP/ICH/172948/2019.
45. Morisseau, C. and B.D. Hammock, *Impact of Soluble Epoxide Hydrolase and Epoxyeicosanoids on Human Health*. Annual Review of Pharmacology and Toxicology, 2013. **53**(1): p. 37-58.
46. Ikei, K.N., et al., *Investigations of human platelet-type 12-lipoxygenase: role of lipoxygenase products in platelet activation*¹[S]. Journal of Lipid Research, 2012. **53**(12): p. 2546-2559.
47. Brash, A.R., A.T. Porter, and R.L. Maas, *Investigation of the selectivity of hydrogen abstraction in the nonenzymatic formation of hydroxyeicosatetraenoic acids and leukotrienes by autoxidation*. Journal of Biological Chemistry, 1985. **260**(7): p. 4210-4216.
48. Hartung, N.M., et al., *Combined Targeted Proteomics and Oxylipin Metabolomics for Monitoring of the COX-2 Pathway*. PROTEOMICS, 2021. **21**(3-4): p. 1900058.
49. Thuresson, E.D., K.M. Lakkides, and W.L. Smith, *Different Catalytically Competent Arrangements of Arachidonic Acid within the Cyclooxygenase Active Site of Prostaglandin Endoperoxide H Synthase-1 Lead to the Formation of Different Oxygenated Products**. Journal of Biological Chemistry, 2000. **275**(12): p. 8501-8507.
50. Giménez-Bastida, J.A., et al., *Residual cyclooxygenase activity of aspirin-acetylated COX-2 forms 15R-prostaglandins that inhibit platelet aggregation*. The FASEB Journal, 2019. **33**(1): p. 1033-1041.
51. Lucido, M.J., et al., *Crystal Structure of Aspirin-Acetylated Human Cyclooxygenase-2: Insight into the Formation of Products with Reversed Stereochemistry*. Biochemistry, 2016. **55**(8): p. 1226-1238.

52. Schebb, N.H., et al., *Formation, Signaling and Occurrence of Specialized Pro-Resolving Lipid Mediators—What is the Evidence so far?* *Frontiers in Pharmacology*, 2022. **13**.
53. Kahnt, A.S., N.H. Schebb, and D. Steinhilber, *Formation of lipoxins and resolvins in human leukocytes*. *Prostaglandins & Other Lipid Mediators*, 2023. **166**: p. 106726.
54. Kühn, H., et al., *Overexpression, purification and characterization of human recombinant 15-lipoxygenase*. *Biochimica et Biophysica Acta (BBA) - Lipids and Lipid Metabolism*, 1993. **1169**(1): p. 80-89.
55. Stenvik Haatveit, Å. and T.V. Hansen, *The biosynthetic pathways of the protectins*. *Prostaglandins & Other Lipid Mediators*, 2023. **169**: p. 106787.
56. Colas, R.A., et al., *Identification and signature profiles for pro-resolving and inflammatory lipid mediators in human tissue*. *American Journal of Physiology-Cell Physiology*, 2014. **307**(1): p. C39-C54.
57. Ostermann, A.I., et al., *Plasma oxylipins respond in a linear dose-response manner with increased intake of EPA and DHA: results from a randomized controlled trial in healthy humans*. *The American Journal of Clinical Nutrition*, 2019. **109**(5): p. 1251-1263.

Table 1. Separation and MS detection parameters of the enantioselective multiple heart-cutting 2D-LC. Shown are the MRM transitions and the MS parameters (declustering potential, DP and collision energy, CE) used for detection, the lower limit of quantification (LLOQ) in the first dimension, retention times, peak width (full width at half maximal height, FWHM) and chromatographic resolution between the enantiomers.

Analyte	m/z Q1	m/z Q3	DP [V]	CE [V]	1D LLOQ		¹ D tR [min] ^b	Peak 1		Peak 2		Resolution ^d
					[nM] ^a	[pg on column] ^a		² D tR [min] ^c	² D FWHM [s]	² D tR [min] ^c	² D FWHM [s]	
9-HODE^e	295.2	171.1	-80	-26	0.14	0.21	20.31	1.646	1.82	1.939	2.30	5.04
13-HODE^e	295.2	195.2	-80	-26	0.25	0.37	20.20	1.547	1.66	2.001	2.21	8.30
9-HOTrE	293.2	171.2	-65	-22	0.50	0.74	17.68	1.565	1.75	1.733	2.06	3.13
13-HOTrE	293.2	195.1	-70	-24	2.5	3.7	18.08	1.326	1.45	1.535	1.82	4.53
13-γ-HOTrE	293.0	193.0	-70	-25	5.0	7.4	18.43	1.025	1.57	1.218	1.78	4.08
5-HETE	319.2	115.2	-60	-21	0.18	0.29	22.30	1.430	1.73	1.525	2.03	1.78
8-HETE	319.2	155.2	-60	-22	0.94	1.5	21.76	1.434	1.82	1.555	1.98	2.26
9-HETE	319.2	167.2	-60	-23	1.33	2.1	22.07	1.429	1.60	1.487	1.59	1.29
11-HETE	319.2	167.2	-60	-23	0.11	0.18	21.44	1.411	1.62	1.514	1.77	2.17
12-HETE	319.2	179.2	-60	-20	0.25	0.40	21.80	1.527	1.80	1.606	2.06	1.44
15-HETE	319.2	219.2	-60	-20	2.2	3.5	20.94	1.455	1.91	1.610	2.05	2.77
16-HETE	319.2	233.1	-65	-20	0.75	1.2	19.76	1.318	1.82	1.477	1.81	3.10
5-HEPE	317.2	115.1	-60	-20	0.30	0.48	19.96	1.282	1.78	1.345	1.95	1.19
8-HEPE	317.2	155.2	-60	-20	0.30	0.48	19.23	1.258	1.66	1.344	1.84	1.73
9-HEPE	317.2	167.0	-40	-19	0.50	0.80	19.61	1.248	1.49	1.307	1.74	1.30
11-HEPE	317.2	167.0	-40	-21	0.31	0.49	19.01	1.294	1.59	1.371	1.85	1.57
12-HEPE	317.2	179.2	-65	-20	0.50	0.80	19.44	1.343	1.59	1.420	1.77	1.61
15-HEPE	317.2	219.2	-60	-20	0.75	1.2	18.90	1.281	1.74	1.336	1.78	1.12
18-HEPE	317.2	259.2	-55	-17	0.75	1.2	18.15	1.249	1.47	1.288	1.57	0.85
4-HDHA	343.2	101.1	-55	-19	0.25	0.43	22.72	1.401	1.60	1.488	1.73	1.86
7-HDHA	343.2	141.2	-55	-19	0.50	0.86	21.97	1.395	1.58	1.455	1.71	1.31
8-HDHA	343.2	189.2	-50	-19	0.29	0.50	22.15	1.376	1.70	1.414	1.87	0.74
10-HDHA	343.2	153.2	-45	-21	0.25	0.43	21.59	1.413	1.62	1.499	1.77	1.79
11-HDHA	343.2	121.1	-45	-20	0.25	0.43	21.86	1.417	1.63	1.470	1.65	1.13
13-HDHA	343.2	193.2	-55	-19	0.25	0.43	21.37	1.433	1.73	1.532	1.72	2.03
14-HDHA	343.2	205.2	-50	-19	0.41	0.71	21.59	1.422	1.63	1.493	1.81	1.46
16-HDHA	343.2	233.2	-55	-19	0.25	0.43	21.10	1.420	1.68	1.469	1.75	1.01
17-HDHA	343.2	201.2	-60	-20	8.5	15	21.21	1.408	1.65	1.460	1.62	1.13
20-HDHA	343.2	241.2	-55	-19	0.50	0.86	20.59	1.344	1.57	1.383	1.61	0.88

^a: The lower limit of quantification (LLOQ) was set to the lowest calibration standards with a signal-to-noise ratio ≥ 5 and accuracy $100\pm 20\%$

^b: Relative standard deviation of the ¹D retention times within one batch was $<0.1\%$ (0.01 min) and $<0.3\%$ (0.06 min) across different batches.

^c: Relative standard deviation of the ²D retention times within one batch was $<0.3\%$ (0.005 min) and $<1\%$ (0.02 min) across different batches

^d: Chromatographic resolution between the enantiomers was calculated as the ratio between the difference of the retention times and the sum of the FWHM of two peaks, multiplied by 1.18.

^e: A longer gradient up to 85% B was used due to the strong retention of these LA-derived oxylipins on the 2D column.

Deducing formation routes of oxylipins by quantitative multiple heart-cutting achiral-chiral 2D-LC-MS

Supporting Information

Nadja Kampschulte, Rebecca Kirchhoff, Ariane Löwen and Nils Helge Schebb*

Chair of Food Chemistry, School of Mathematics and Natural Sciences,
University of Wuppertal

*contact information of the corresponding author:

Nils Helge Schebb

Chair of Food Chemistry, Faculty of Mathematics and Natural Sciences, University of Wuppertal
Gausstrasse 20, 42119 Wuppertal

Email: nils@schebb-web.de

Phone: +49-202-439-3457

Table of content

Additional method parameters	2
Isobaric interferences in MRM-detection of oxylipins	6
Impact of the mobile phase on the enantioselective separation of oxylipins	9
Optimization of active solvent modulation	10
Limit of quantification in the second dimension	11
Chiral separation of vicinal dihydroxy-FA	11
Enantioselective 2D-LC-separation of EPA, DHA, ARA linoleic acid linoleic acid-derived oxylipin isomers	13
COX-Inhibition in HCA-7 cells	19
Lack of separation of dihydroxy-fatty acid diastereomers by reversed-phase chromatography .	20
Detection of dihydroxy-EPA and -DHA isomers using different transitions in ESI(-)-MS/MS	21
Enantioselective analysis of 10,17-DiHDHA isomers	23

Additional method parameters

Chemicals and biological materials

Hydroxy-FA, racemic mixtures of vicinal *threo*-dihydroxy-FA and all other oxylipin standards and isotopically labeled oxylipins were purchased from Cayman Chemical (Ann Arbor, Michigan, United States) or Larodan (Solna, Sweden) [1, 2]. 18(*R*)-HEPE and 18(*S*)-HEPE were synthesized in house as described [3]. LC-MS-grade acetonitrile, methanol, *iso*-propanol, and acetic acid were obtained from Fisher Scientific (Schwerte, Germany). Ultra-pure water ($R=18.2\text{ M}\Omega$) was generated with a Barnstead Genpure Pro system (Thermo Fisher Scientific, Langenselbold, Germany). Fetal calf serum (superior standardized) was purchased from Biochrom (Berlin, Germany). Dulbecco's Modified Eagle's Medium (DMEM), L-glutamine and all other cell culture reagents and chemicals were purchased from Sigma Aldrich (Schnelldorf, Germany). HCA-7 cells were obtained from the European Collection of Cell Cultures (ECACC, Salisbury, UK). HEK293T cells inducibly expressing *ALOX15* were a kind gift from the laboratory of Dieter Steinhilber, Goethe University Frankfurt, Germany. Pooled human EDTA plasma as well as pooled human serum from healthy individuals was generated as described [2], approved by the ethics committee of the University of Wuppertal and in accordance with the guidelines of the Declaration of Helsinki. In brief, blood was collected in EDTA-monovettes, immediately centrifuged for 10 min at 1200 *g* and 4 °C. The supernatant plasma was carefully collected. Plasma of different subjects was pooled, gently mixed, aliquoted and frozen at -80 °C immediately afterwards. Of note, the plasma and serum were not obtained from the same donors. Human pooled EDTA plasma, which showed high concentrations of lipid autoxidation products presumably resulting from processing and storing in a non-frozen state for an extended period of time (oxidized plasma), was purchased from BioIVT (West Sussex, United Kingdom).

Time-dependent multiple heart-cutting

The oxylipins eluting from the first, i.e. RP dimension were collected in the 2D sample loops by time-dependent multiple heart-cutting. The cut-times were determined based on the retention time of the oxylipins in the 1D analysis. The start of the heart-cut was set 0.13 min earlier than the peak maximum in the 1D-LC-MS/MS signal. The correction of 0.13 minutes results from i) the void time between the 1D column and the MS detector (i.e. 0.07 min), which was determined by the implementation of a UV detector in the flow path immediately after the 1D column and the measurement of oxylipins in a concentration which was detectable in both, UV- and MS/MS and ii) the approximate half peak width (i.e. 0.065 min) in order to start with the heart-cutting at the beginning of the respective peak. Before every batch measured in the 2D-LC set up, a 1D run was carried out in order to determine the current retention times and thus cut times.

Table S1. Exemplary sample table for the multiple heart-cutting of oxylipins. 17 oxylipins are collected in 14 heart cuts with “smart peak parking”. The cut start time was set 0.13 min earlier than the time of the peak maximum in an 1D measurement as described above.

oxylipin	1D retention time [min]	1D cut start [min]	Cut no.	deck	loop	2D run start [min]
14,15-DiHETE	14.74	14.61	1	A	1	14.79
14,15-DiHETrE*	16.41	16.30	2	B	1	18.96
19,20-DiHEPE*	16.46	16.98	3	B	2	17.16
16,17-DiHDPE	17.11	17.99	4	A	1	30.24
18-HEPE	18.12	18.73	5	A	2	28.44
12-HEPE	19.41	19.28	6	A	3	26.64
5-HEPE	19.93	19.80	7	A	4	24.84
15-HETE	20.92	20.79	8	A	5	23.04
17-HDHA	21.19	21.06	9	A	6	21.24
14-HDHA	21.57	21.44	10	B	1	39.41
10-HDHA	21.57	21.63	11	B	2	37.61
8-HETE*	21.74	21.82	12	B	3	35.81
12-HETE*	21.77	22.15	13	B	4	34.01
7-HDHA	21.95	22.57	14	B	5	32.21
5-HETE	22.28					
4-HDHA	22.70					

* the set cut time of these analytes is a compromise in order to collect both of the closely eluting oxylipins in one loop.

Internal standards

Table S2: Assignment of the isotope-labeled oxylipins used as internal standard for quantification to the analytes.

oxylipin	internal standard	oxylipin	internal standard
9-HODE	² H ₄ -9-HODE	11-HEPE	² H ₈ -15-HETE
13-HODE	² H ₄ -13-HODE	12-HEPE	² H ₈ -15-HETE
9,10-DiHOME	² H ₄ -9,10-DiHOME	15-HEPE	² H ₈ -15-HETE
12,13-DiHOME	² H ₄ -9,10-DiHOME	18-HEPE	² H ₈ -15-HETE
9-HOTrE	² H ₄ -13-HODE	5,6-DiHETE	² H ₄ -LTB ₄
13-HOTrE	² H ₄ -13-HODE	8,9-DiHETE	² H ₄ -LTB ₄
9,10-DiHODE	² H ₄ -9,10-DiHOME	11,12-DiHETE	² H ₄ -LTB ₄
12,13-DiHODE	² H ₄ -9,10-DiHOME	14,15-DiHETE	² H ₄ -LTB ₄
15,16-DiHODE	² H ₄ -9,10-DiHOME	17,18-DiHETE	² H ₄ -LTB ₄
13-γ-HOTrE	² H ₄ -LTB ₄	4-HDHA	² H ₈ -5-HETE
5-HETE	² H ₈ -5-HETE	7-HDHA	² H ₈ -5-HETE
8-HETE	² H ₈ -12-HETE	8-HDHA	² H ₈ -5-HETE
9-HETE	² H ₈ -5-HETE	10-HDHA	² H ₈ -12-HETE
11-HETE	² H ₈ -12-HETE	11-HDHA	² H ₈ -5-HETE
12-HETE	² H ₈ -12-HETE	13-HDHA	² H ₈ -12-HETE
15-HETE	² H ₈ -15-HETE	14-HDHA	² H ₈ -12-HETE
16-HETE	² H ₈ -15-HETE	16-HDHA	² H ₈ -15-HETE
5,6-DiHETrE	² H ₁₁ -11,12-DiHETrE	17-HDHA	² H ₈ -15-HETE
8,9-DiHETrE	² H ₁₁ -11,12-DiHETrE	20-HDHA	² H ₈ -15-HETE
11,12-DiHETrE	² H ₁₁ -11,12-DiHETrE	7,8-DiHDPE	² H ₁₁ -11,12-DiHETrE
14,15-DiHETrE	² H ₁₁ -11,12-DiHETrE	10,11-DiHDPE	² H ₁₁ -11,12-DiHETrE
5-HEPE	² H ₈ -15-HETE	13,14-DiHDPE	² H ₁₁ -11,12-DiHETrE
8-HEPE	² H ₈ -15-HETE	16,17-DiHDPE	² H ₁₁ -11,12-DiHETrE
9-HEPE	² H ₈ -15-HETE	19,20-DiHDPE	² H ₁₁ -11,12-DiHETrE

Table S3: MS detection parameters and 1D retention times of isotope-labeled oxylipins (internal standards) used for the quantification of hydroxy- and dihydroxy-FA.

internal standard	retention time [min]	m/z Q1	m/z Q3	DP [V]	CE [V]
² H ₄ -13-HODE	20.07	299.2	198.1	-60	-22
² H ₄ -9-HODE	20.19	299.2	172.3	-80	-26
² H ₄ -9,10-DiHOME	15.57	317.2	203.4	-80	-29
² H ₄ -LTB ₄	14.42	339.2	197.2	-55	-23
² H ₈ -5-HETE	22.18	327.2	116.1	-60	-21
² H ₈ -12-HETE	21.65	327.2	184.2	-65	-22
² H ₈ -15-HETE	20.75	327.2	226.0	-70	-20
² H ₁₁ -11,12-DiHETrE	17.10	348.2	167.2	-60	-27

Peak annotation

The elution order of hydroxy-FA on amylose-based chiral selectors apparently follows a trend whereby the *R*-enantiomer elutes earlier than the *S*-enantiomer. This is reported in a large number of studies using both NP and RP conditions [4-7], as well as SFC [8]. This is in line with the enantiopure standards analyzed here (Fig. 2, Fig. S4). Consistently the (*R,R*)-isomer of a vicinal dihydroxy-FA elutes before the (*S,S*)-enantiomer [9]. However, for individual pairs of hydroxy-FA enantiomers a reversed elution order is described [4, 10], which is not supported by other studies [4-7]. *S*-enantiomers of saturated FA hydroxylated at C3 position elute earlier than their *R*-enantiomers on an amylose phase under RP conditions [11]. Therefore the two enantiomers' peaks can only be annotated to the *R*- and *S*-isomer, if a (bio)synthetic standard with a significant EF is available. Otherwise, only a tentative characterization can be deduced.

In order to deduce the *R* and *S* configuration, an enantioselective enzymatic transesterification of racemic mixtures of hydroxy-FA was carried out. 0.3 nmol hydroxy-FA were dissolved in 1 mL *n*-hexane and 10 μ L vinyl acetate as well as 5 mg Amano-Lipase-PS from *Burkholderia cepacia* were added [12]. The reaction was carried out in an incubation shaker (1000 rpm) at 37 °C for 30 h. The reaction was terminated by filtration through a 0.1 μ m PVDF centrifugal filter and extraction of the oxylipins from the hexane phase was done by means of solid-phase extraction using amino propyl material under normal phase conditions as described [13]. As the enzyme selectively accepts only the *R*-isomer as a substrate forming the acetylated *R*-hydroxy-FA, an excess of the *S*-isomer remains in the reaction mixture, enabling assignment of stereoisomers following chiral separation.

Isobaric interferences in MRM-detection of oxylipins

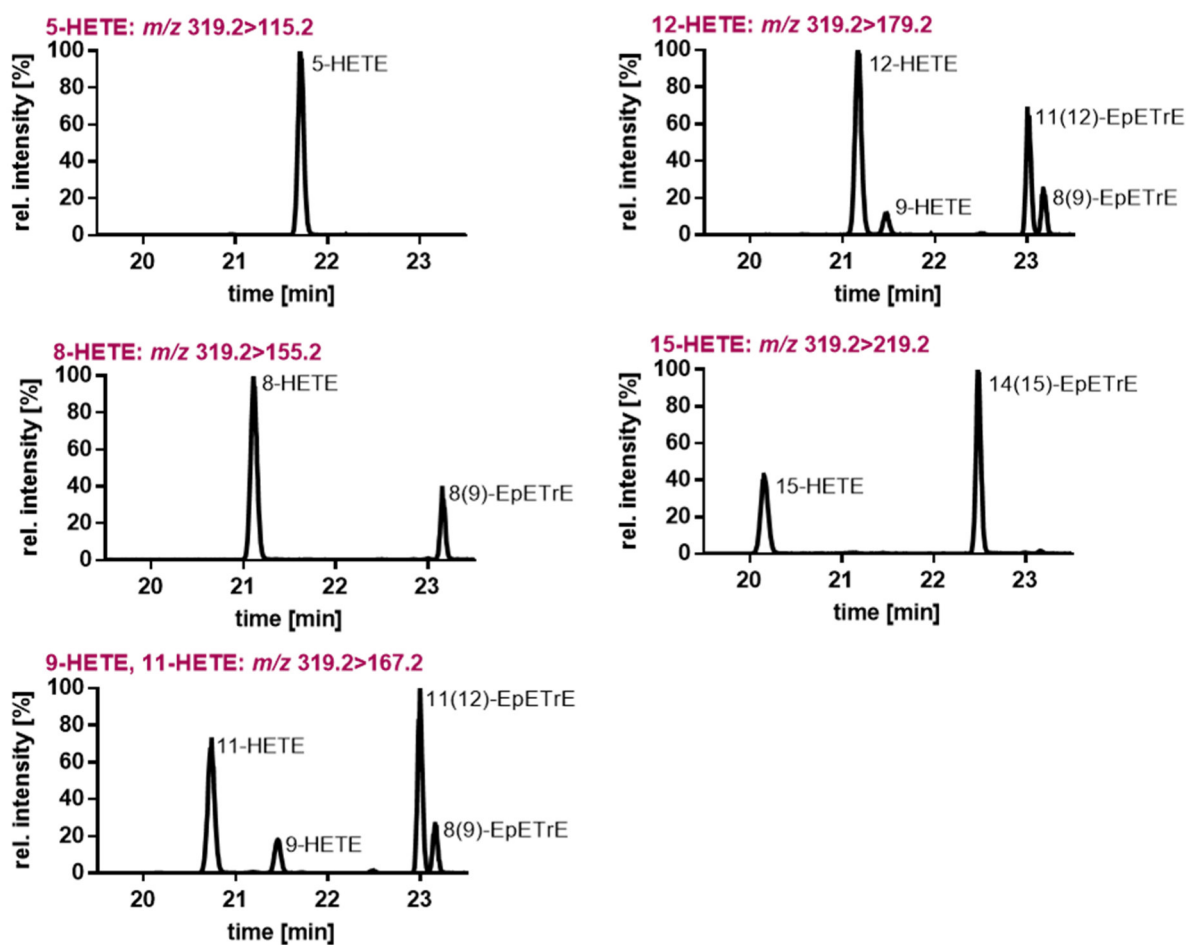


Figure S1A: 1D separation of a multianalyte standard of oxylipins (250 nM). Shown are the MRM transitions of the arachidonic acid (ARA)-derived oxylipins 5-HETE, 12-HETE, 8-HETE, 15-HETE and 9-HETE/11-HETE. Several of the isobaric hydroxy-ARA and epoxy-ARA give rise to the same fragment ions. Thus none of the MS transitions are specific for a single oxylipin and chromatographic separation is required for a selective analysis.

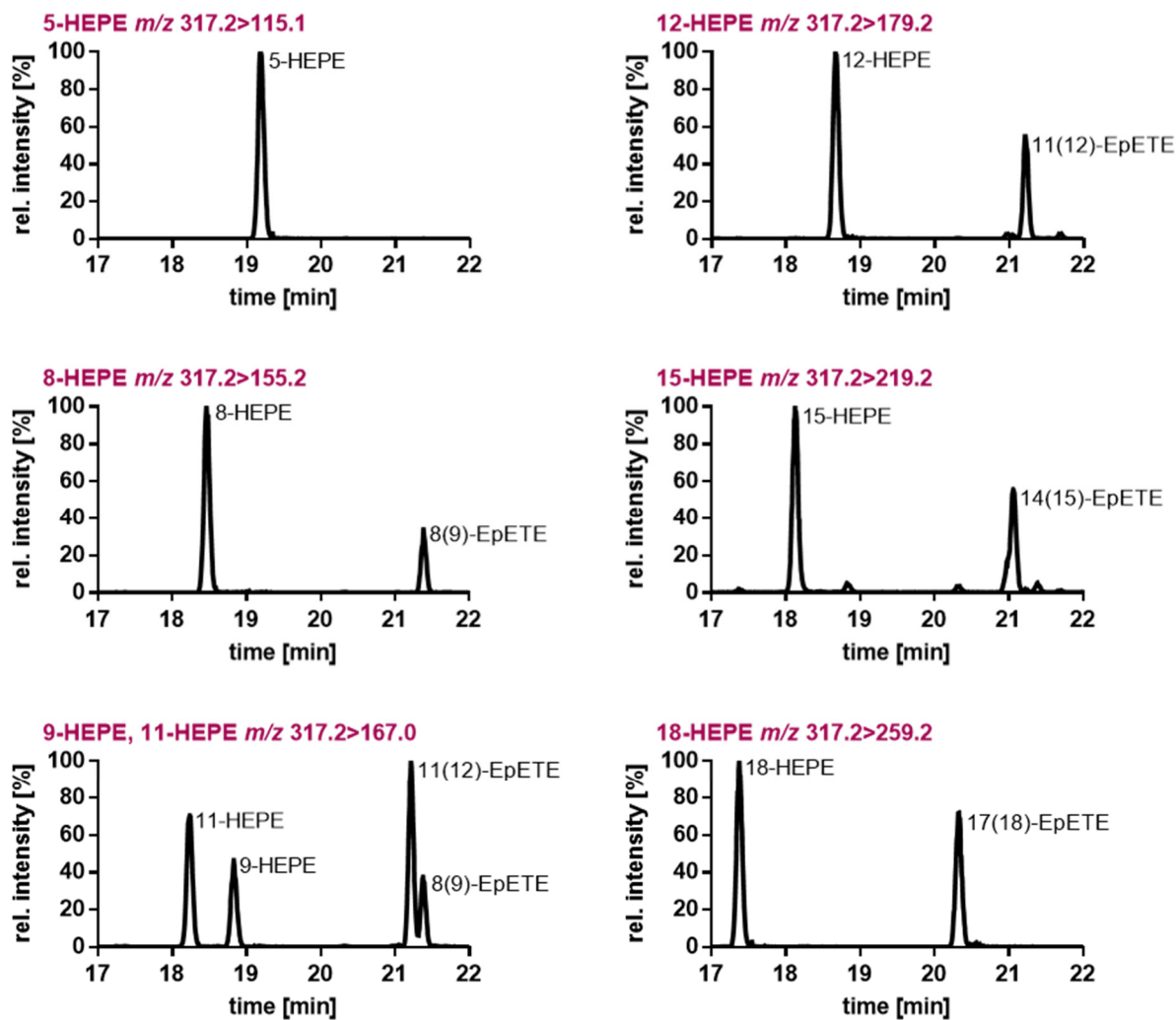


Figure S1B: 1D separation of a multianalyte standard of oxylipins (250 nM). Shown are the MRM transitions of the eicosapentaenoic acid (EPA)-derived oxylipins 5-HEPE, 12-HEPE, 8-HEPE, 15-HEPE and 9-HEPE/11-HEPE and 18-HEPE. Several of the isobaric hydroxy-EPA and epoxy-EPA give rise to the same fragment ions. Thus, none of the MS transitions are specific for a single oxylipin and chromatographic separation is required for a selective analysis.

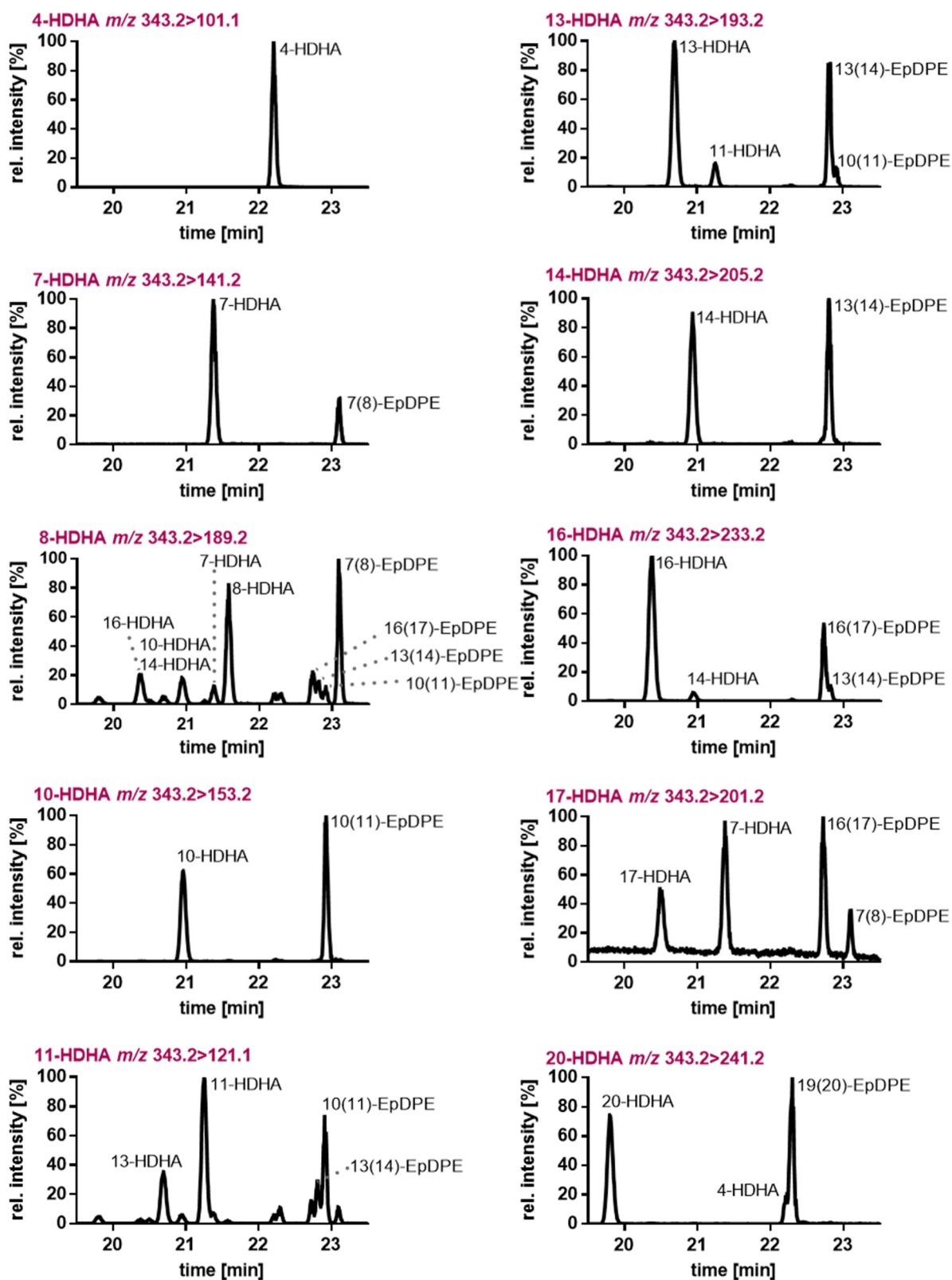


Figure S1C: 1D separation of a multianalyte standard of oxylipins (250 nM). Shown are the MRM transitions of the docosahexaenoic acid (DHA)-derived oxylipins 4-HDHA, 7-HDHA, 8-HDHA, 10-HDHA, 11-HDHA, 13-HDHA, 14-HDHA, 16-HDHA, 17-HDHA and 20-HDHA. Several of the isobaric hydroxy-DHA and epoxy-DHA give rise to the same fragment ions. and the MS transitions. Thus, none of the MS transitions are specific for a single oxylipin and chromatographic separation is required for a selective analysis.

Impact of the mobile phase on the enantioselective separation of oxylipins

Table S4: Impact of the mobile phase on the separation of oxylipin enantiomers^a. Shown are the chromatographic separation factor (selectivity) and the peak resolution for each pair of enantiomers.

Analyte	Solvent A	Solvent B	Selectivity ^b	Resolution ^c
14,15-DiHETrE	water/acetonitrile 80/20 (v/v)	acetonitrile	1.046	1.34
	water/methanol 80/20 (v/v)	acetonitrile/methanol 80/20 (v/v)	1.019	0.60
	water/ <i>iso</i> -propanol 80/20 (v/v)	acetonitrile/ <i>iso</i> -propanol 80/20 (v/v)	1.012	< 0.45
14,15-DiHETE	water/acetonitrile 80/20 (v/v)	acetonitrile	1.039	0.96
	water/methanol 80/20 (v/v)	acetonitrile/methanol 80/20 (v/v)	1.015	0.49
	water/ <i>iso</i> -propanol 80/20 (v/v)	acetonitrile/ <i>iso</i> -propanol 80/20 (v/v)	1	< 0.45
16,17-DiHDPE	water/acetonitrile 80/20 (v/v)	acetonitrile	1.028	0.62
	water/methanol 80/20 (v/v)	acetonitrile/methanol 80/20 (v/v)	1.011	< 0.45
	water/ <i>iso</i> -propanol 80/20 (v/v)	acetonitrile/ <i>iso</i> -propanol 80/20 (v/v)	1	< 0.45
15-HETE	water/acetonitrile 80/20 (v/v)	acetonitrile	1.058	2.09
	water/methanol 80/20 (v/v)	acetonitrile/methanol 80/20 (v/v)	1.042	1.81
	water/ <i>iso</i> -propanol 80/20 (v/v)	acetonitrile/ <i>iso</i> -propanol 80/20 (v/v)	1.015	0.51
18-HEPE	water/acetonitrile 80/20 (v/v)	acetonitrile	1.014	0.46
	water/methanol 80/20 (v/v)	acetonitrile/methanol 80/20 (v/v)	1.011	< 0.45
	water/ <i>iso</i> -propanol 80/20 (v/v)	acetonitrile/ <i>iso</i> -propanol 80/20 (v/v)	1	< 0.45
17-HDHA	water/acetonitrile 80/20 (v/v)	acetonitrile	1.016	0.52
	water/methanol 80/20 (v/v)	acetonitrile/methanol 80/20 (v/v)	1.013	0.53
	water/ <i>iso</i> -propanol 80/20 (v/v)	acetonitrile/ <i>iso</i> -propanol 80/20 (v/v)	1	< 0.45

^a Gradient in the second dimension: 0.00 min–0.40 min 10% B, 0.40 min – 2.0 min linear 10 to 90% B, 2.00-2.30, 90% B. All solvents contained 0.1% acetic acid.

^b selectivity α was calculated as $\alpha = \frac{t'_{R2}}{t'_{R1}}$ with t'_R as the net retention time ($t_R - t_{void}$) of the respective peak.

^c Peak resolution was calculated as $R = 1.18 * \frac{t_{R2} - t_{R1}}{FWHM_1 + FWHM_2}$

Optimization of active solvent modulation

Active solvent modulation (ASM) describes a feature by which the solvent flow used for the transfer of a heart-cut into the second dimension is split in order to adjust the solvent composition (Fig. S2A). Here, ASM was used at the beginning of the ²D gradient in order to improve 2D separation. In the ASM setup, only a third of the ²D flow is passing through the sample loop and thus, a dilution of the stored ¹D solvent is achieved. This results in reduced elution strength during the transfer of the analytes to the ²D column (Fig. S2A). During the ASM, the ²D pump delivers 95% of solvent A, i.e. solvent with low elution power. After this, a linear gradient from 35% to 70% B is used to separate the oxylipin enantiomers in the second dimension. ASM remarkably improves the separation as shown exemplary of the critical separation pair 18(*R,S*)-HEPE (Fig. 2). Considering the loop volume (40 μL), the flow rate of 0.9 mL/min and the ASM factor of 3, the injection of the heart-cut loop content onto the second dimension requires 0.14 min. Accordingly, after 0.14 min, the ASM was switched off. Longer ASM did not yield further improvement of the separation (Fig. S2B). Interestingly, for several applications longer ASM times are used, for example, 1.8× capillary flushes have been described for reaching an optimal peak shape when size exclusion chromatography is coupled to RP-LC [14]. ASM was initially developed to improve compatibility between ¹D and ²D separations [15], and is frequently used in HILIC×RPLC platforms, e.g. to reduce a breakthrough in the ²D analysis caused by solvent strength miss matches [16-18]. Here, we show that ASM is also highly beneficial in a RP-chiral-RP MHC setup improving separation.

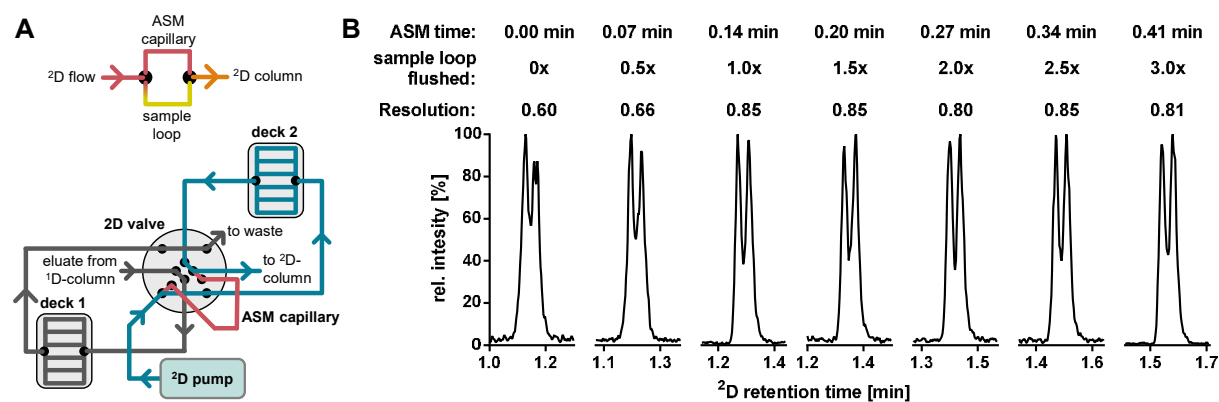


Figure S2. Active solvent modulation improves chiral separation of oxylipin enantiomers. A Setup of the active solvent modulation (ASM) within the multiple heart-cutting two-dimensional LC system. By splitting the flow of the ²D pump, a dilution (dilution factor 3) of the ¹D solvent in the sample loop is achieved, yielding lower elution strength at the beginning of the ²D gradient. **B** Chiral separation of the injection of a racemic 18-HEPE solution (50 nM) with variation of the duration of ASM. ²D gradient elution was carried out with a flow rate of 0.9 mL/min.

Limit of quantification in the second dimension

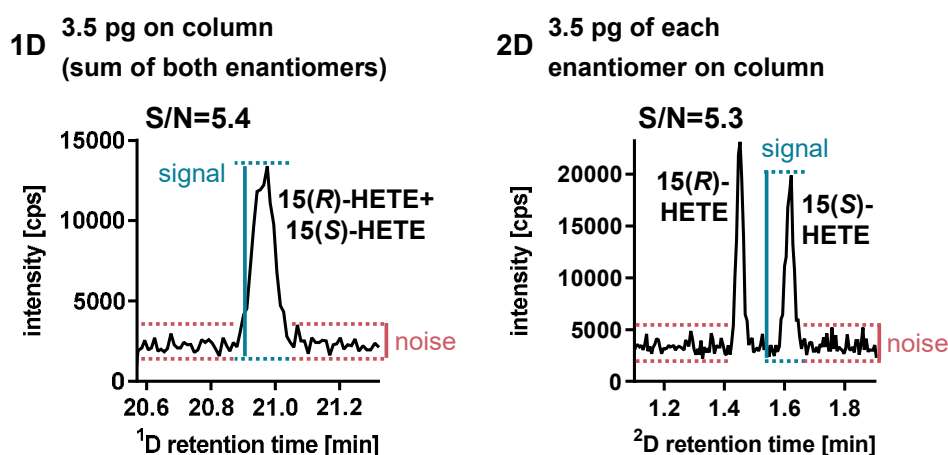


Figure S3. Lower limit of quantification of the 1D- and 2D-analysis of 15-HETE. LC-ESI(-)-MS/MS chromatogram of an injection of a 2.2 nM racemic 15-HETE standard (3.5 pg on column) measured by 1D-RP-LC-MS/MS and 2D chromatogram following heart-cutting and chiral separation of an 4.4 nM racemic 15-HETE standard (7.0 pg total, i.e. 3.5 pg of each enantiomer on column). In the chromatograms the determination of the signal-to-noise ratio (S/N) is illustrated, showing an (S/N) ≥ 5 . In combination with an accuracy of 100% \pm 20% this concentration is set as lower limit of quantification (LOQ).

Chiral separation of vicinal dihydroxy-FA

In addition to the chiral separation of hydroxy-FA, this achiral-chiral MHC-2D-LC-MS/MS method enables the enantioselective separation of 16 vicinal *threo*-dihydroxy-FA, which has been only described for ARA-derived DiHETrE [9] and 5,6-DiHETE [7] before. These oxylipins result from the (soluble epoxide hydrolase-catalyzed) hydrolysis of *cis*-epoxy-FA, which in turn are products of cytochrome-P450-monooxygenase (CYP)-catalyzed epoxidation of unsaturated FA. The two enantiomers of *cis* epoxy-FA are formed to a different extent by CYP enzymes, and are hydrolyzed by sEH at different rates [4]. Taking the biological activity of epoxy-PUFA, but also of the dihydroxy-PUFA into account, information of the concentration of the enantiomers could be of high biological importance. With achiral-chiral MHC-2D-LC, all four vicinal dihydroxy-ARA derivatives (DiHETrE), four DiHETE- and three DiHDPE isomer pairs are separated, as well as five C18-dihydroxy-FA (Tab. S5, Fig. S4). Enantiomers of vicinal dihydroxy-FA which carry the hydroxy-groups in the middle of the carbon chain of the fatty acids are well separated, while the enantiomers of the positional isomers carrying the stereocenters close to the methyl- or the carboxy-end are less well resolved (Tab. S5, Fig. S4).

Table S5. Separation and MS detection parameters of the enantioselective multiple heart-cutting 2D-LC analysis of vicinal dihydroxy-FA. Shown are the MRM transitions and the MS parameters (declustering potential, DP and collision energy, CE) used for detection, the lower limit of quantification (LLOQ) in the first dimension, retention times, peak width (full width at half maximal height, FWHM) and chromatographic resolution between the enantiomers.

Analyte	m/z Q1	m/z Q3	DP [V]	CE [V]	1D LLOQ		¹ D tR [min] ^b	Peak 1		Peak 2		Resolution ^d
					[nM] ^a	[pg on column] ^a		² D tR [min] ^c	² D FWHM [s]	² D tR [min] ^c	² D FWHM [s]	
9,10-DiHOME^e	313.2	201.2	-80	-29	0.05	0.08	15.67	1.478	1.95	1.828	3.43	4.60
12,13-DiHOME^e	313.2	183.2	-80	-30	0.06	0.09	15.20	1.507	2.15	1.653	2.84	2.07
9,10-DiHODE	311.2	201.2	-65	-27	0.10	0.16	13.47	1.294	2.18	1.677	4.20	4.25
12,13-DiHODE	311.2	183.1	-80	-30	1.0	1.6	13.57	1.209	2.00	1.384	3.01	2.47
15,16-DiHODE	311.2	223.2	-80	-29	0.91	1.4	13.42	1.266	2.19	1.329	2.48	0.95
5,6-DiHETrE	337.2	145.1	-70	-26	0.25	0.42	18.89	1.190	1.67	1.276	1.73	1.79
8,9-DiHETrE	337.2	127.1	-70	-30	0.17	0.29	17.93	1.215	1.81	1.364	2.40	2.51
11,12-DiHETrE	337.2	167.1	-65	-26	0.16	0.27	17.27	1.266	1.80	1.397	2.34	2.24
14,15-DiHETrE	337.2	207.1	-65	-25	0.10	0.17	16.44	1.301	1.79	1.403	2.30	1.75
5,6-DiHETE	335.2	115.1	-60	-21	1.5	2.5	16.22	1.042	1.46	1.114	1.32	1.81
8,9-DiHETE	335.2	127.1	-65	-26	0.25	0.42	15.39	1.062	1.54	1.163	1.94	2.06
11,12-DiHETE	335.2	167.1	-65	-26	0.25	0.42	14.99	1.136	1.72	1.213	2.09	1.44
14,15-DiHETE	335.3	207.2	-65	-25	0.25	0.42	14.76	1.106	1.70	1.174	1.97	1.32
17,18-DiHETE	335.3	247.2	-65	-24	0.55	0.93	14.13	1.114 ^f	2.64 ^g	1.114 ^f	2.64 ^g	<0.5
7,8-DiHDPE	361.2	113.1	-65	-24	0.75	1.4	18.67	1.182	3.67 ^g	1.210	3.67 ^g	<0.5
10,11-DiHDPE	361.2	153.2	-65	-24	0.25	0.45	17.82	1.232	1.68	1.339	2.28	1.92
13,14-DiHDPE	361.2	193.2	-65	-24	0.25	0.45	17.43	1.263	1.86	1.358	2.32	1.62
16,17-DiHDPE	361.2	233.2	-65	-24	0.25	0.45	17.14	1.236	1.65	1.300	2.02	1.23
19,20-DiHDPE	361.2	273.2	-65	-24	0.10	0.18	16.49	1.208	3.71 ^g	1.236	3.71 ^g	<0.5

^a: The lower limit of quantification (LLOQ) was set to the lowest calibration standards with a signal-to-noise ratio ≥ 5 and accuracy $100\pm 20\%$

^b: Relative standard deviation of the ¹D retention times within one batch was $<0.1\%$ (0.01 min) and $<0.3\%$ (0.06 min) across different batches.

^c: Relative standard deviation of the ²D retention times within one batch was $<0.3\%$ (0.005 min) and $<1\%$ (0.02 min) across different batches

^d: Chromatographic resolution between the enantiomers was calculated as the ratio between the difference of the retention times and the sum of the FWHM of two peaks, multiplied by 1.18.

^e: A longer gradient up to 85% B was used due to the strong retention of these LA-derived oxylipins on the 2D column.

^f: Peaks could not be distinguished.

^g: No separation of the enantiomers at half maximal height.

Enantioselective 2D-LC-separation of EPA, DHA, ARA linoleic acid linoleic acid-derived oxylipin isomers

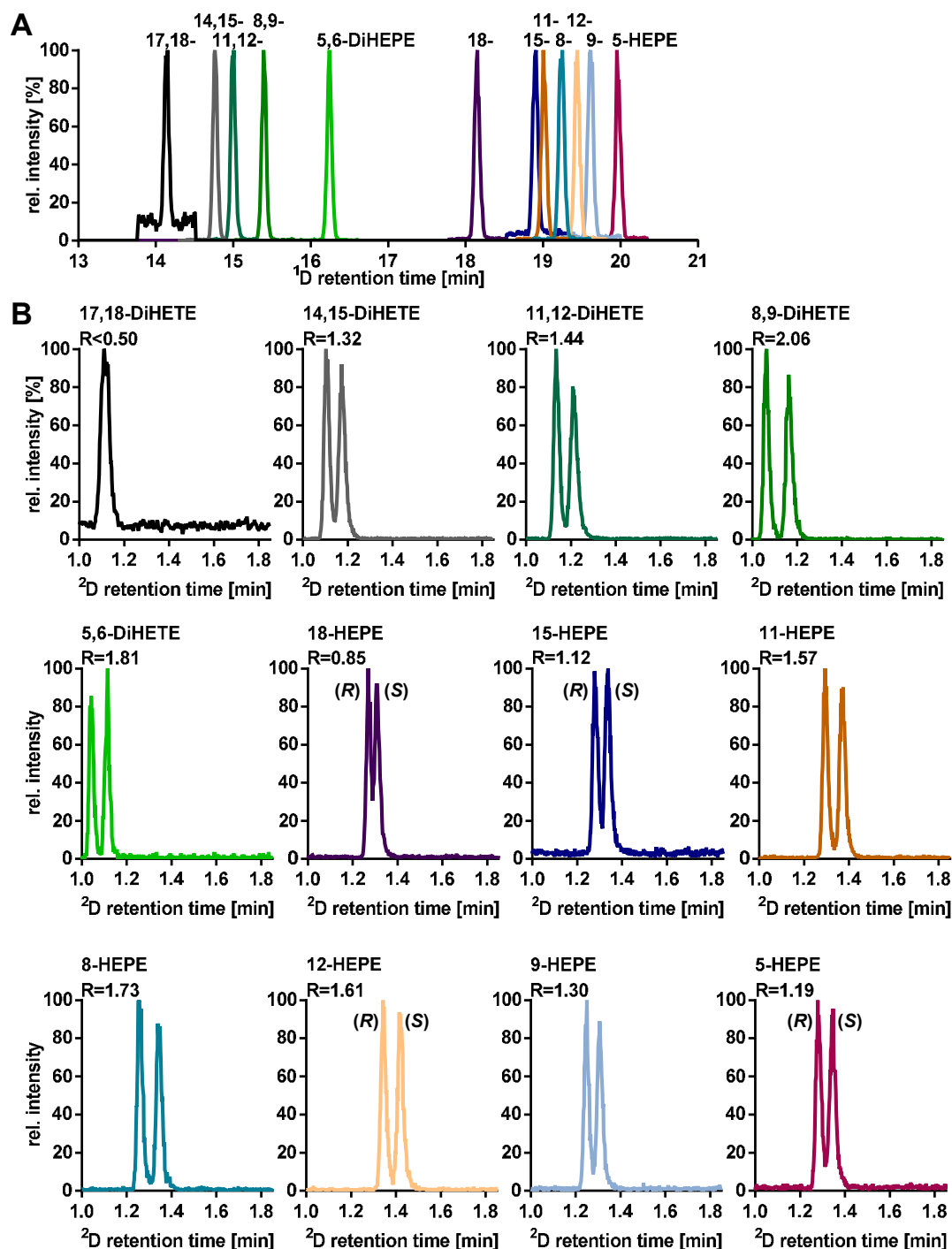


Figure S4A: Chiral separation of eicosapentaenoic acid (EPA)-derived oxylipins by means of 2D-LC-MS/MS. A ¹D chromatogram using a RP18 stationary phase (2.1 mm × 150 mm, 1.8 μm particles) and acidified water and acetonitrile with methanol as solvents. **B** Multiple heart cutting ²D chromatograms following chiral separation using an amylose-based tris(3,5-dimethyl-phenylcarbamate) phase (3.0 mm × 50 mm, < 2 μm particles) and acidified water and acetonitrile as eluents. A sufficient separation of the enantiomers of seven HEPE regioisomers is achieved, and with the exception of 17,18-DiHETE, also the vicinal dihydroxy-derivatives of EPA can be analyzed enantioselectively for the first time. 18-HEPE is a critical separation pair among the hydroxy-FA. Detection in both, 1D- and 2D-LC was carried by a triple quadrupole MS in MRM following ionization by electrospray ionization in negative mode. The separation of a racemic multi analyte oxylipin standard (50 nM) is shown.

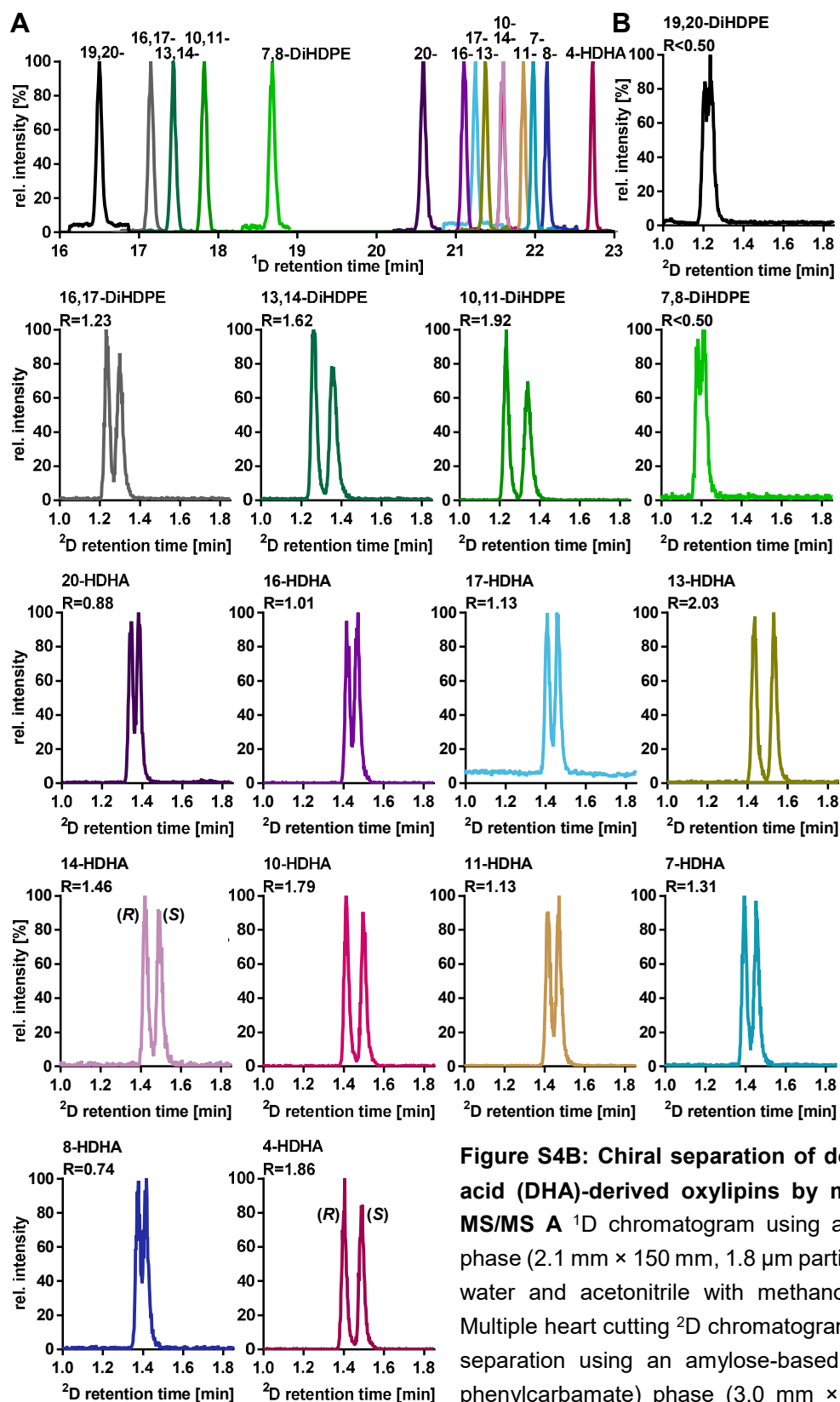


Figure S4B: Chiral separation of docosa-hexaenoic acid (DHA)-derived oxylipins by means of 2D-LC-MS/MS **A** ¹D chromatogram using a RP18 stationary phase (2.1 mm × 150 mm, 1.8 μm particles) and acidified water and acetonitrile with methanol as solvents. **B** Multiple heart cutting ²D chromatograms following chiral separation using an amylose-based tris(3,5-dimethylphenylcarbamate) phase (3.0 mm × 50 mm, < 2 μm particles) and acidified water and acetonitrile as eluents. A sufficient separation of the enantiomers of ten HDHA regioisomers is achieved, and with the exception of 19,20- and 7,8-DiHDPE, also the vicinal dihydroxy-derivatives of DHA can be analyzed enantioselectively for the first time. Detection in both, 1D- and 2D-LC was carried by a triple quadrupole MS in MRM following ionization by electrospray ionization in negative mode. The separation of a racemic multi analyte oxylipin standard (50 nM) is shown.

A sufficient separation of the enantiomers of ten HDHA regioisomers is achieved, and with the exception of 19,20- and 7,8-DiHDPE, also the vicinal dihydroxy-derivatives of DHA can be analyzed enantioselectively for the first time. Detection in both, 1D- and 2D-LC was carried by a triple quadrupole MS in MRM following ionization by electrospray ionization in negative mode. The separation of a racemic multi analyte oxylipin standard (50 nM) is shown.

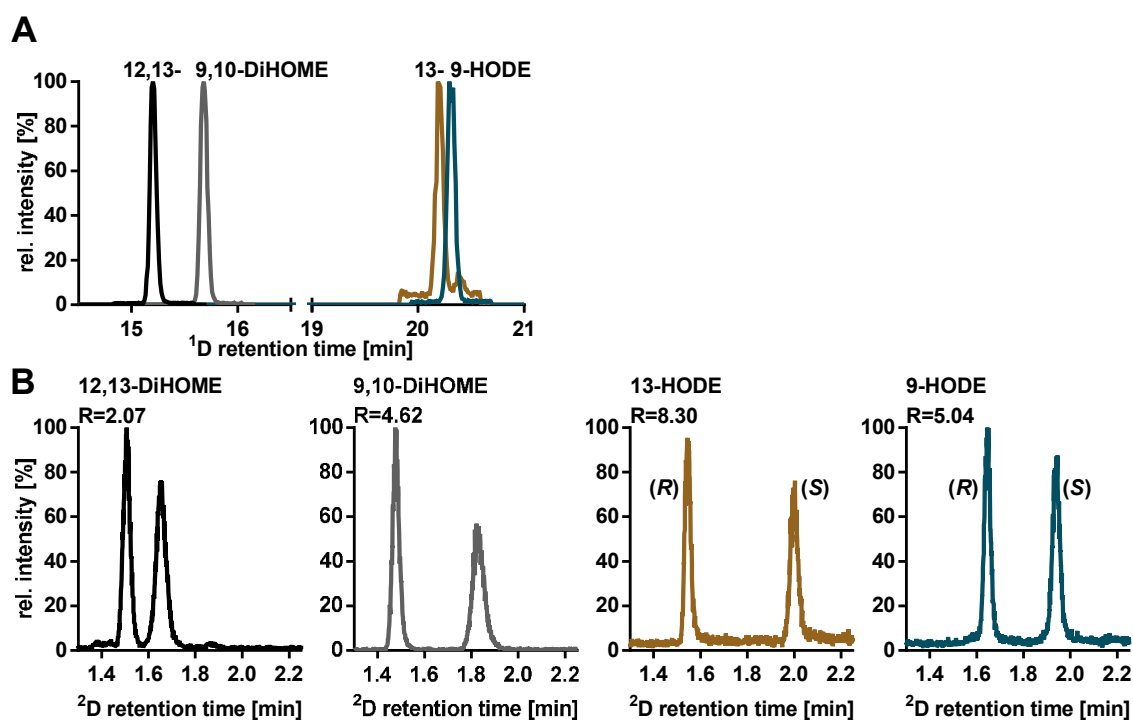


Figure S4C: Chiral separation of linoleic acid (LA)-derived oxylipins by means of 2D-LC-MS/MS.

A ¹D chromatogram using a RP18 stationary phase (2.1 mm × 150 mm, 1.8 μm particles) and acidified water and acetonitrile with methanol as solvents. **B** Multiple heart cutting ²D chromatograms following chiral separation using an amylose-based tris(3,5-dimethyl-phenylcarbamate) phase (3.0 mm × 50 mm, < 2 μm particles) and acidified water and acetonitrile as eluents. A gradient up to 85% B was used in the ²D due to the strong retention of these LA-derived oxylipins on the 2D column. Baseline separation was achieved for both linoleic acid-derived dihydroxy-FA all well as both HODE regioisomers. Detection in both, 1D- and 2D-LC was carried by a triple quadrupole MS in MRM following ionization by electrospray ionization in negative mode. The separation of a racemic multi analyte oxylipin standard (50 nM) is shown.

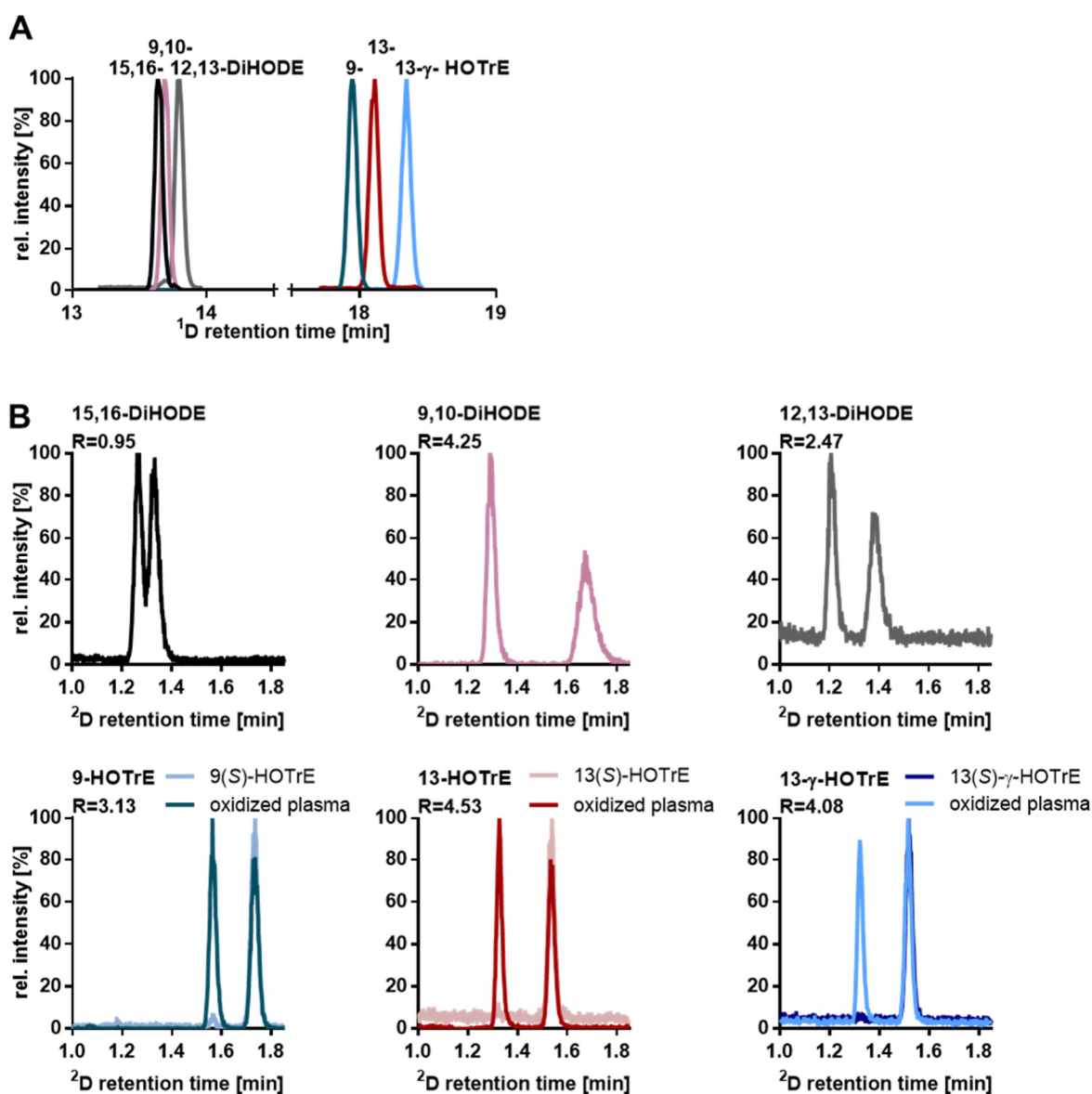


Figure S4D: Chiral separation of α -linolenic acid (ALA)- and γ -linolenic acid-derived oxylipins by means of 2D-LC-MS/MS. **A** ¹D chromatogram using a RP18 stationary phase (2.1 mm \times 150 mm, 1.8 μ m particles) and acidified water and acetonitrile with methanol as solvents. **B** Multiple heart cutting ²D chromatograms following chiral separation using an amylose-based tris(3,5-dimethyl-phenylcarbamate) phase (3.0 mm \times 50 mm, < 2 μ m particles) and acidified water and acetonitrile as eluents. Six linolenic acid-derived octadecanoids are enantioselectively separated in the second dimension. Detection in both, 1D- and 2D-LC was carried by a triple quadrupole MS in MRM following ionization by electrospray ionization in negative mode. The separation of a multi analyte oxylipin standard (50 nM) containing racemic mixtures of DiHODE and S-enantiomers of HOTrE is shown. Additionally, separation of an oxidized plasma sample, containing racemic mixtures of HOTrE, is shown.

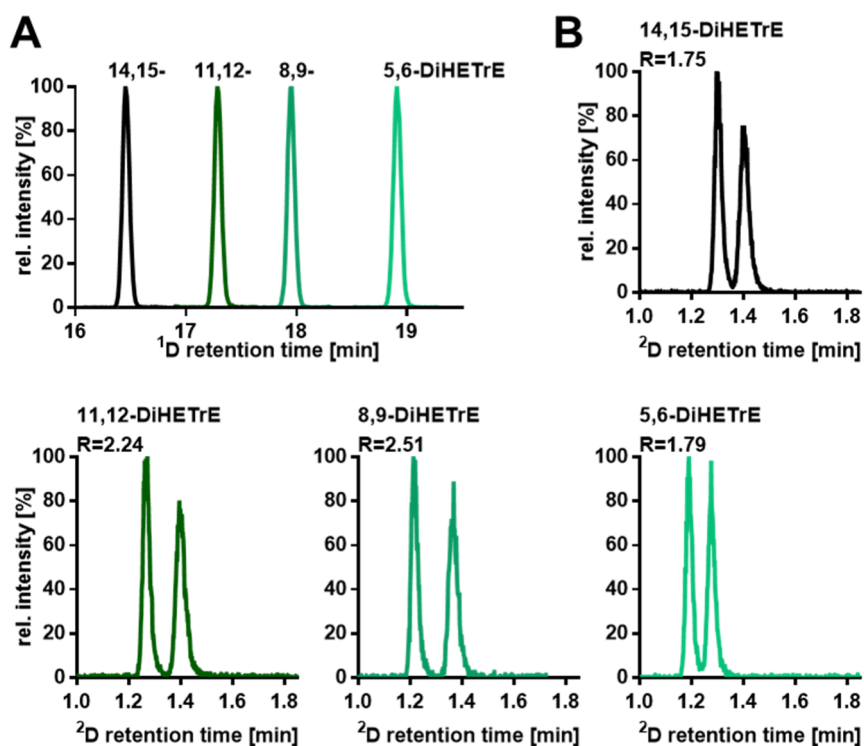


Figure S4E: Chiral separation of arachidonic acid (ARA)-derived vicinal dihydroxy-FA by means of 2D-LC-MS/MS. **A** 1D chromatogram using a RP18 stationary phase (2.1 mm × 150 mm, 1.8 μm particles) and acidified water and acetonitrile with methanol as solvents. **B** Multiple heart cutting 2D chromatograms following chiral separation using an amylose-based tris(3,5-dimethyl-phenylcarbamate) phase (3.0 mm × 50 mm, < 2 μm particles) and acidified water and acetonitrile as eluents. Detection in both, 1D- and 2D-LC was carried by a triple quadrupole MS in MRM following ionization by electrospray ionization in negative mode. The separation of a racemic multi analyte oxylipin standard (50 nM) is shown. Note: the separation of the ARA-derived hydroxy-FA is shown in Fig. 2 of the manuscript.

Table S6. Oxylipins concentration and enantiomeric fractions (EF) in plasma, serum and oxidized plasma and intra- and inter batch variation. Oxylipin extraction and analysis from three aliquots was carried out on three different days. Oxylipins were quantified by means of 1D LC-MS/MS and enantiomeric fractions (EF) of the enantiomeric mixtures were determined following 2D chiral separation. Shown is the mean \pm SD (n=4).

		plasma			serum			oxidized plasma		
		conc. [nM]	RSD	EF (Peak 1 : Peak 2) [%]	conc. [nM]	RSD	EF (Peak 1 : Peak 2) [%]	conc. [nM]	RSD	EF (Peak 1 : Peak 2) [%]
5-HETE	day 1	0.73 \pm 0.08	11%	34:66 (\pm 2)	1.88 \pm 0.15	8%	16:84 (\pm 1)	1250 \pm 70	6%	41:59 (\pm 1)
	day 2	0.74 \pm 0.03	4%	35:65 (\pm 2)	1.93 \pm 0.16	8%	17:83 (\pm 1)	1430 \pm 150	11%	41:59 (\pm 1)
	day 3	0.78 \pm 0.06	8%	32:68 (\pm 2)	2.21 \pm 0.15	7%	16:84 (\pm 1)	1470 \pm 80	6%	41:59 (\pm 1)
	interbatch	0.75 \pm 0.03	3%	34:66 (\pm 2)	2.01 \pm 0.18	9%	16:84 (\pm 1)	1400 \pm 110	8%	41:59 (\pm 1)
8-HETE	day 1	0.20 \pm 0.05	23%	51:49 (\pm 2)	1.47 \pm 0.10	7%	73:27 (\pm 1)	251 \pm 15	6%	54:46 (\pm 1)
	day 2	0.19 \pm 0.02	11%	47:53 (\pm 2)	1.53 \pm 0.04	2%	69:31 (\pm 2)	250 \pm 12	5%	55:45 (\pm 1)
	day 3	0.17 \pm 0.01	8%	50:50 (\pm 4)	1.4 \pm 0.04	3%	72:28 (\pm 4)	244 \pm 21	9%	53:47 (\pm 1)
	interbatch	0.19 \pm 0.01	7%	49:51 (\pm 2)	1.47 \pm 0.06	4%	71:29 (\pm 2)	248 \pm 4	2%	54:46 (\pm 1)
12-HETE	day 1	1.45 \pm 0.08	6%	22:78 (\pm 1)	216 \pm 15	7%	0:100 (\pm 1)	372 \pm 23	6%	48:52 (\pm 1)
	day 2	1.44 \pm 0.03	2%	22:78 (\pm 2)	206 \pm 6	3%	0:100 (\pm 1)	384 \pm 15	4%	48:52 (\pm 1)
	day 3	1.33 \pm 0.10	8%	23:77 (\pm 2)	206 \pm 5	2%	0:100 (\pm 1)	364 \pm 27	7%	49:51 (\pm 1)
	interbatch	1.41 \pm 0.07	5%	22:78 (\pm 1)	209 \pm 6	3%	0:100 (\pm 1)	373 \pm 10	3%	48:52 (\pm 1)
15-HETE	day 1	1.01 \pm 0.04	4%	34:66 (\pm 4)	7.0 \pm 0.4	5%	36:64 (\pm 1)	510 \pm 30	6%	48:52 (\pm 1)
	day 2	0.95 \pm 0.03	3%	37:63 (\pm 3)	6.8 \pm 0.2	3%	36:64 (\pm 1)	510 \pm 40	8%	48:52 (\pm 1)
	day 3	0.92 \pm 0.03	3%	34:66 (\pm 2)	6.69 \pm 0.12	2%	36:64 (\pm 1)	477 \pm 24	5%	48:52 (\pm 1)
	interbatch	0.96 \pm 0.05	5%	35:65 (\pm 2)	6.8 \pm 0.1	2%	36:64 (\pm 1)	497 \pm 17	4%	48:52 (\pm 1)
14,15-DiHETrE	day 1	0.64 \pm 0.03	4%	11:89 (\pm 1)	0.42 \pm 0.02	4%	9:91 (\pm 1)	0.82 \pm 0.06	8%	16:84 (\pm 1)
	day 2	0.64 \pm 0.03	5%	11:89 (\pm 1)	0.43 \pm 0.01	3%	10:90 (\pm 2)	0.90 \pm 0.06	7%	15:85 (\pm 1)
	day 3	0.64 \pm 0.03	4%	11:89 (\pm 1)	0.43 \pm 0.01	3%	11:89 (\pm 1)	0.83 \pm 0.01	1%	17:83 (\pm 1)
	interbatch	0.64 \pm 0.01	1%	11:89 (\pm 1)	0.43 \pm 0.01	1%	10:90 (\pm 1)	0.85 \pm 0.05	5%	16:84 (\pm 1)
5-HEPE	day 1	0.13 \pm 0.01	3%	23:77 (\pm 4)	0.12 \pm 0.01	6%	23:77 (\pm 8)	149 \pm 9	6%	42:58 (\pm 1)
	day 2	0.12 \pm 0.01	3%	20:80 (\pm 1)	0.11 \pm 0.01	3%	28:72 (\pm 7)	151 \pm 13	9%	42:58 (\pm 1)
	day 3	0.12 \pm 0.01	5%	21:79 (\pm 4)	0.11 \pm 0.01	3%	27:73 (\pm 3)	148 \pm 5	4%	44:56 (\pm 1)
	interbatch	0.12 \pm 0.01	5%	21:79 (\pm 1)	0.11 \pm 0.01	8%	26:74 (\pm 3)	149 \pm 2	1%	43:57 (\pm 1)
18-HEPE	day 1	0.23 \pm 0.02	7%	64:36 (\pm 4)	0.57 \pm 0.02	4%	20:80 (\pm 5)	11.1 \pm 0.6	6%	34:66 (\pm 1)
	day 2	0.25 \pm 0.02	8%	61:39 (\pm 11)	0.58 \pm 0.05	9%	26:74 (\pm 3)	12.2 \pm 0.9	8%	27:73 (\pm 2)
	day 3	0.25 \pm 0.01	6%	67:33 (\pm 4)	0.58 \pm 0.02	3%	25:75 (\pm 2)	11.8 \pm 0.2	1%	37:63 (\pm 1)
	interbatch	0.24 \pm 0.01	4%	64:36 (\pm 3)	0.58 \pm 0.01	1%	23:77 (\pm 3)	11.7 \pm 0.6	5%	32:68 (\pm 5)
4-HDHA	day 1	0.20 \pm 0.02	11%	44:56 (\pm 2)	0.25 \pm 0.02	7%	37:63 (\pm 2)	150 \pm 12	8%	45:55 (\pm 1)
	day 2	0.22 \pm 0.01	4%	44:56 (\pm 3)	0.28 \pm 0.02	7%	42:58 (\pm 3)	166 \pm 22	13%	44:56 (\pm 1)
	day 3	0.20 \pm 0.02	12%	44:56 (\pm 3)	0.26 \pm 0.03	10%	37:63 (\pm 2)	162 \pm 6	4%	45:55 (\pm 1)
	interbatch	0.21 \pm 0.01	6%	44:56 (\pm 1)	0.27 \pm 0.01	5%	39:61 (\pm 3)	159 \pm 9	5%	45:55 (\pm 1)
10-HDHA	day 1	0.10 \pm 0.01	8%	50:50 (\pm 7)	0.73 \pm 0.06	8%	56:44 (\pm 3)	96 \pm 7	7%	53:47 (\pm 1)
	day 2	0.09 \pm 0.01	12%	46:54 (\pm 6)	0.70 \pm 0.06	8%	55:45 (\pm 3)	97 \pm 5	5%	53:47 (\pm 1)
	day 3	0.08 \pm 0.01	5%	42:58 (\pm 3)	0.70 \pm 0.02	3%	56:44 (\pm 2)	93 \pm 7	7%	54:46 (\pm 1)
	interbatch	0.09 \pm 0.01	7%	46:54 (\pm 4)	0.71 \pm 0.02	3%	55:45 (\pm 1)	96 \pm 2	2%	54:46 (\pm 1)

COX-Inhibition in HCA-7 cells

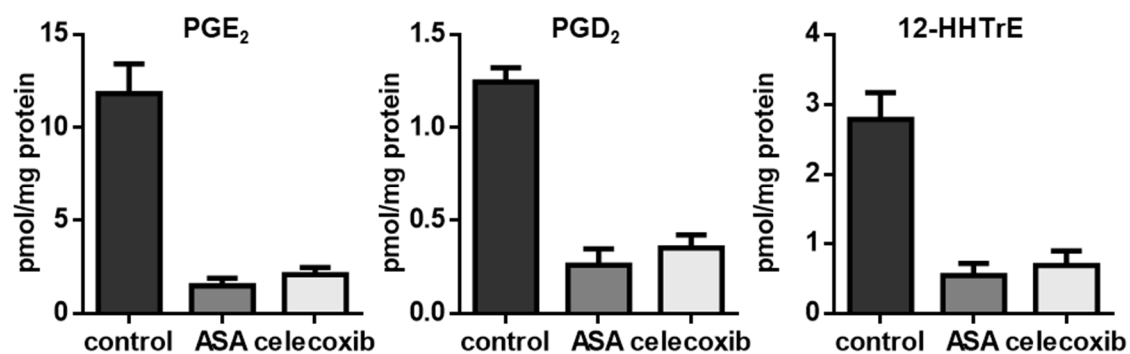


Figure S5: Inhibition of COX-2 catalyzed oxylipin formation in HCA-7 cells by acetylsalicylic acid (ASA) or celecoxib. HCA-7 cells were incubated with 100 μ M ASA or 10 μ M celecoxib for 24 h and PGE₂, PGD₂ and 12-HHTrE were quantified in the cells by means of LC-MS/MS. Shown is the mean \pm SD; n=4

Lack of separation of dihydroxy-fatty acid diastereomers by reversed-phase chromatography

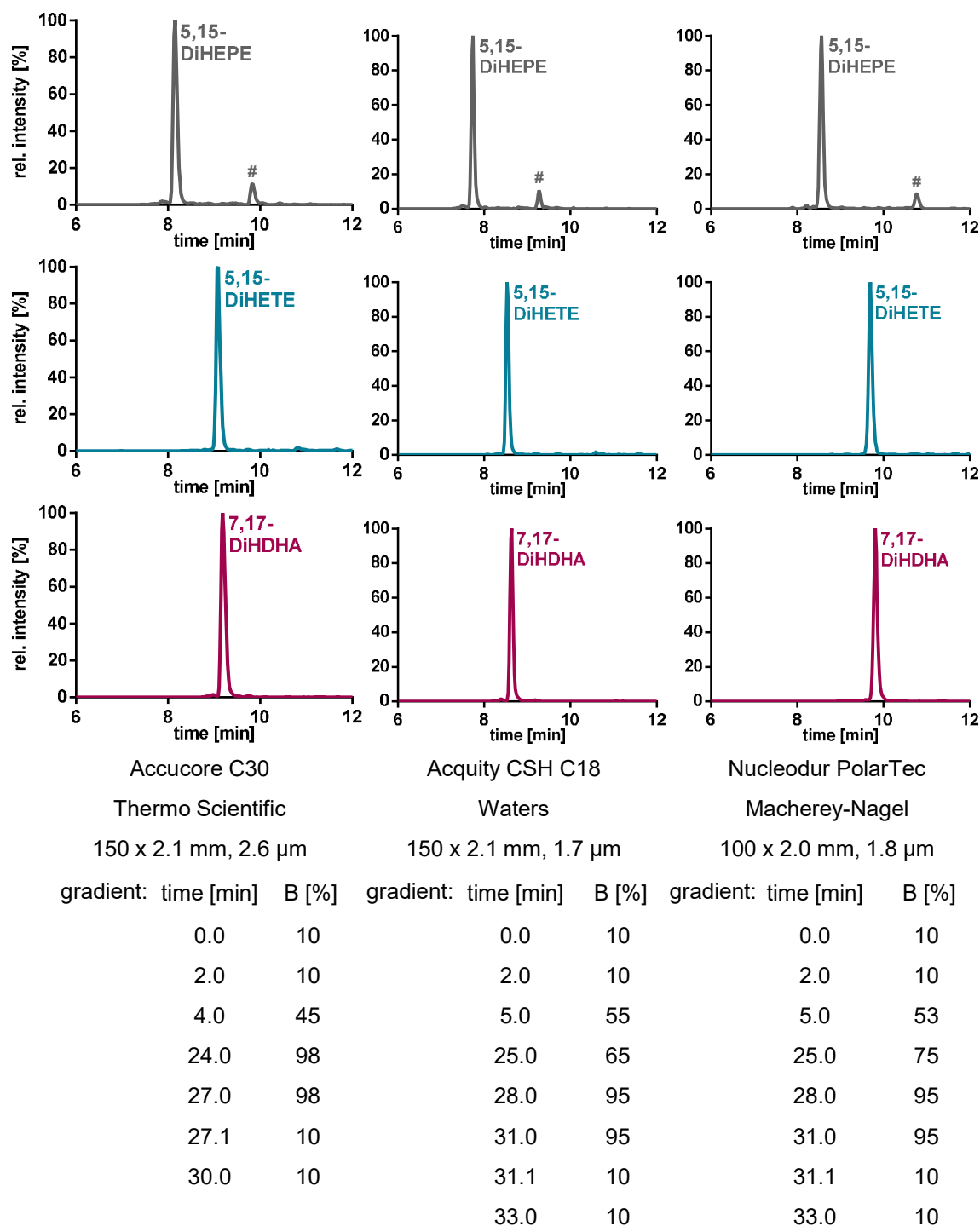


Figure S6: 1D Reversed-phase chromatograms of enzymatically formed diastereomeric 5(*R/S*),15(*S*)-DiHETE, 5(*R/S*)-,15(*S*)-DiHEPE and 7(*R/S*),17(*S*)-DiHDHA using the indicated stationary phases. Acidified water and acetonitrile with methanol were used as mobile phase. Separation as carried out with a Vanquish Horizon LC system and oxylipins were detected following negative electrospray ionization with an hybrid quadrupole-orbitrap mass spectrometer (Q Exactive HF) operated in full MS data-dependent MS²-mode. Shown are the XIC of *m/z* 335.2228 (DiHETE), *m/z* 333.2071 (DiHEPE), and *m/z* 359.2228 (DiHDHA) (Mass accuracy \pm 5 ppm). #: This peak shows a different MS² spectrum and thus is an isobaric interference and not 5,15-DiHEPE.

Figure S7: Comparison of two MRM transitions for the detection of dihydroxy-EPA and -DHA. A Structure of 5,15-DiHEPE and suggested sites of fragmentation of leading to the two ions monitored in MRM. **B** Signals of both SRM transitions following 1D RP separation of a 100 nM 5(*S*),15(*S*)-DiHEPE standard and extracted oxidized plasma. **C** Signals of both MRM transitions following ²D chiral separation of a 100 nM 5(*S*),15(*S*)-DiHEPE standard and extracted oxidized plasma. **D** Structure of 7,17-DiHDHA and suggested sites of fragmentation leading to the two ions monitored in MRM. **E** Signals of both MRM transitions following 1D RP separation of a 100 nM 7(*S*),17(*S*)-DiHDHA standard and extracted oxidized plasma. **F** Signals of both MRM transitions following ²D chiral separation of a 100 nM 7(*S*),17(*S*)-DiHDHA standard and extracted oxidized plasma. The dotted lines in panels B and E indicate the time of the heart-cutting.

*: Stereo configuration of these isomers is estimated based on elution order.

In order to increase specificity and to support that the signals of the stereo isomers of 7,17-DiHDHA and 5,15-DiHEPE are actually caused by these compounds alone and not by other compounds such as positional isomers (e.g. oxylipins which carry the hydroxyl functions at other positions within the fatty acid chain) two MRM transitions of these dihydroxy-oxylipins were recorded. In the 1D RP analysis of the respective (*S*),(*S*) standard compound as well as the ²D signal following chiral chromatography, the transitions each show the expected number of signals – one single clear peak –with a constant intensity ratio between the two transitions (Fig. S7). Monitoring oxidized fatty acids with the selected transitions in an extract of autoxidized plasma following RP also yields one peak with the same retention time and transitions' intensity ratio. However, several other peaks are detected originating from isobaric compounds with different hydroxylation patterns and/or double bond positions and configurations. Of note, none of these matches the standard's intensity ratio of the two transitions. Achiral-chiral-MHC-2D-LC-MS/MS enables here the analysis of stereo isomers without inferences of the large number of further positional isomers. Chiral ²D analysis of the of 7,17-DiHDHA and 5,15-DiHEPE peaks shows that all four stereoisomers of the two compounds are found in oxidized plasma, with an intensity ratio of the two transitions identical to that of the standard.

Enantioselective analysis of 10,17-DiHDHA isomers

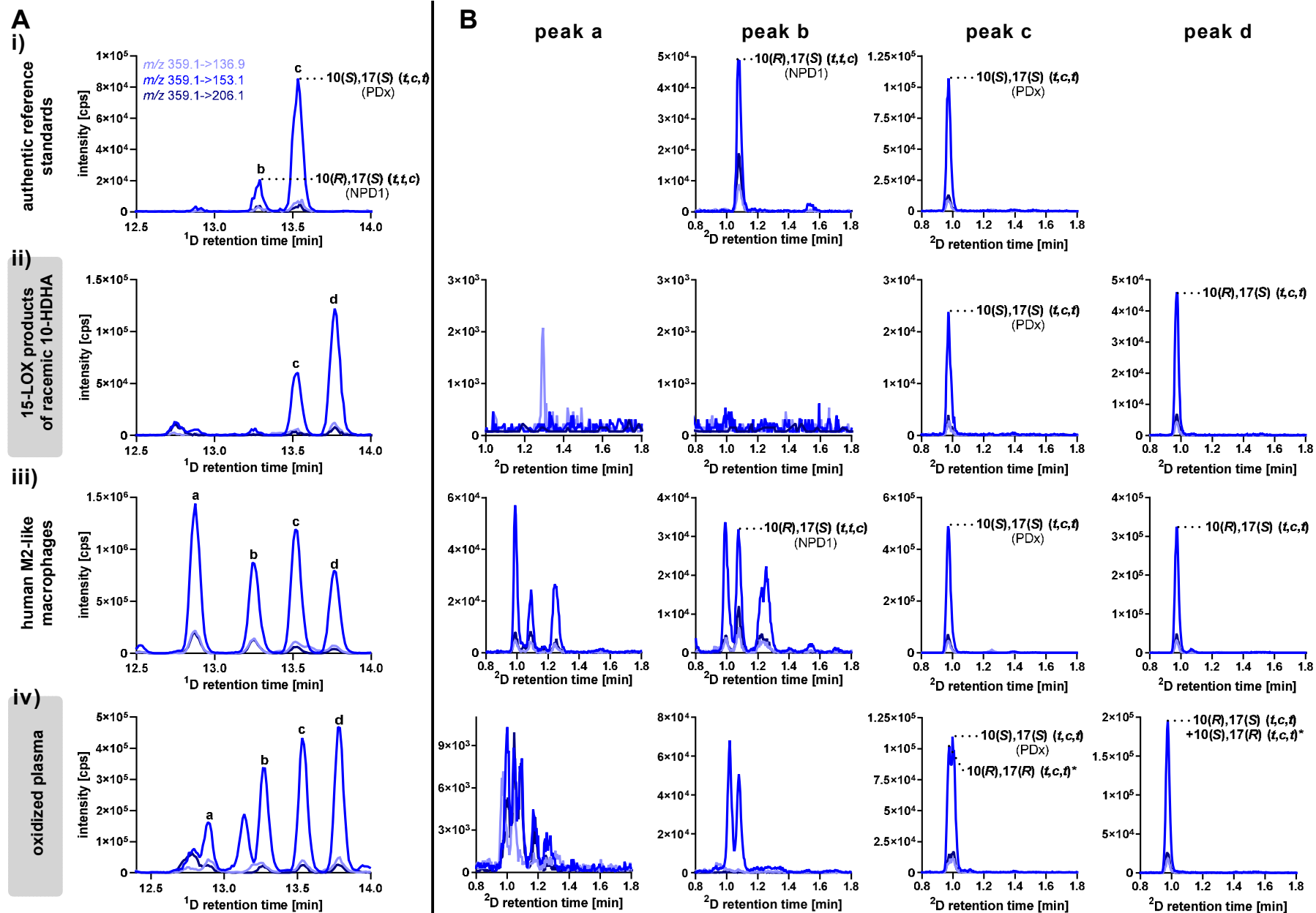


Figure S8. Analysis of 10,17-DiHDHA isomers by enantioselective heart-cutting 2D-LC. **A** 1D RP chromatograms (MRM signals) of **(i)** a standard mixture (50 nM) containing 10(*S*),17(*S*)-dihydroxy-4(*Z*),7(*Z*),11(*E*),13(*Z*),15(*E*),19(*Z*)-docosahexaenoic acid (10(*S*),17(*S*)-DiHDHA; PDX) and 10(*R*),17(*S*)-dihydroxy-4(*Z*),7(*Z*),11(*E*),13(*E*),15(*Z*),19(*Z*)-docosahexaenoic acid (NPD1), **(ii)** 10(*R/S*),17(*S*)-DiHDHA, which was generated by conversion of 10(*R,S*)-HDHA by human 15-LOX, **(iii)** human M2-like macrophages supplemented with DHA in the cultivation medium and **(iv)** oxidized (commercial) human plasma. **B** 2D chromatograms (MRM signals) following chiral separation of the peaks a–d collected by multiple heart-cutting from the first (RP) dimension.

*: Stereo configuration of these isomers is estimated based on elution order.

Analogous to the formation of 7,17-DiHDHA from 7-HDHA by 15-LOX, 10,17-DiHDHA can be formed from 10-HDHA. The resulting product carries a conjugated *trans, cis, trans* (*t,c,t*) triene system. One of the stereoisomers of these structures (10(*S*),17(*S*)-DiHDHA), is called protectin DX in the literature [19]. For other configuration isomers of 10,17-DiHDHA formation pathways *via* 17-hydroperoxy-DHA and 16,17-*trans*-epoxy-DHA are hypothesized, eventually yielding 10,17-DiHDHA carrying a conjugated *trans, trans, cis* (*t,t,c*) triene system. The 10(*R*),17(*S*)-Isomer of this structure is named protectin D1 [20, 21].

Formation by 15-LOX catalyzed conversion of racemic 10(*R,S*)-HDHA and subsequent RP analysis of the diastereomeric 10(*R/S*),17(*S*)-DiHDHA (*t,c,t*) revealed that a chromatographic separation of these diastereomers is possible by means of RP-LC (Fig. S8A, peaks c and d). Furthermore, two peaks matching the retention time and the MRM transitions' intensity ratio of the diastereomers are found in human M2-like macrophages as well as in oxidized plasma. 10,17-DiHDHA with a (*t,t,c*) configuration was not detected in the enzyme incubations. On the contrary, two additional peaks with similar intensity ratios of the MRM transitions were detected in both, macrophages and autoxidized plasma (Fig. S8A, peaks a and b). One of these matches the retention time of the 10(*R*),17(*S*)-DiHDHA (*t,t,c*) (peak b). We assume that the other peak can be assigned to the diastereoisomer of this oxylipin (peak a).

Chiral analysis following multiple heart-cutting revealed that in human M2-like macrophages only the 10(*S*),17(*S*)-DiHDHA (*t,c,t*) and not its enantiomer 10(*R*),17(*R*)-DiHDHA (*t,c,t*) is present, while the two are detected in the oxidized plasma (Fig. S8B). It can be concluded that 10,17-DiHDHA (*t,c,t*) in macrophages is formed by 15-LOX catalytic activity from (racemic) 10-HDHA. However, no chiral separation was achieved for 10(*R*),17(*S*)-DiHDHA (*t,c,t*) and its enantiomer 10(*S*),17(*R*)-DiHDHA (*t,c,t*), as both isomers should be present in oxidized plasma. Nonetheless, the 10(*S*),17(*S*)-DiHDHA (*t,c,t*) "PDX" can be reliably distinguished from its stereo isomers.

Stereoselective separation of the tentative 10,17-DiHDHA (*t,t,c*) isomers revealed that the single peak in the RP chromatogram consists of a large number of different isomers: The chromatograms of the chiral second dimension of macrophages and oxidized plasma extracts show clear differences – but both contain several isomers. Without stereoselective analysis, it is therefore not possible to reliably report "NPD1". As earlier reported this is also observed by differences in the intensity ratios of two transitions of the peak of the standard compared to the peak of the isomer mixture in biological samples [22, 23].

Moreover it should be noted that the 10(*R*),17(*S*)-DiHDHA (*t,t,c*) in the achiral-chiral-MHC-2D-LC-MS chromatogram of M2-like macrophages is only one of at least three components and not the dominating

compound. Thus, we assume it is formed by non-controlled autoxidation and consider a controlled enzymatic formation in the macrophages to be unlikely.

References

1. Hartung, N.M., et al., *Development of a quantitative proteomics approach for cyclooxygenases and lipoxygenases in parallel to quantitative oxylipin analysis allowing the comprehensive investigation of the arachidonic acid cascade*. Analytical and Bioanalytical Chemistry, 2023. **415**(5): p. 913-933.
2. Koch, E., et al., *Stability of oxylipins during plasma generation and long-term storage*. Talanta, 2020. **217**: p. 121074.
3. Kutzner, L., et al., *Human lipoxygenase isoforms form complex patterns of double and triple oxygenated compounds from eicosapentaenoic acid*. Biochim Biophys Acta Mol Cell Biol Lipids, 2020. **1865**(12): p. 158806.
4. Blum, M., et al., *Chiral lipidomics of monoepoxy and monohydroxy metabolites derived from long-chain polyunsaturated fatty acids[S]*. Journal of Lipid Research, 2019. **60**(1): p. 135-148.
5. Bayer, M., A. Mosandl, and D. Thaçi, *Improved enantioselective analysis of polyunsaturated hydroxy fatty acids in psoriatic skin scales using high-performance liquid chromatography*. Journal of Chromatography B, 2005. **819**(2): p. 323-328.
6. Schneider, C., et al., *Enantiomeric Separation of Hydroxy and Hydroperoxy Eicosanoids by Chiral Column Chromatography*, in *Methods in Enzymology*. 2007, Academic Press. p. 145-157.
7. Cebo, M., et al., *Enantioselective ultra-high performance liquid chromatography-tandem mass spectrometry method based on sub-2 μ m particle polysaccharide column for chiral separation of oxylipins and its application for the analysis of autoxidized fatty acids and platelet releasates*. Journal of Chromatography A, 2020. **1624**: p. 461206.
8. Quaranta, A., et al., *Development of a Chiral Supercritical Fluid Chromatography–Tandem Mass Spectrometry and Reversed-Phase Liquid Chromatography–Tandem Mass Spectrometry Platform for the Quantitative Metabolic Profiling of Octadecanoid Oxylipins*. Analytical Chemistry, 2022. **94**(42): p. 14618-14626.
9. Capdevila, J.H., et al., *Resolution of dihydroxyeicosanoates and of dihydroxyeicosatrienoates by chiral phase chromatography*. Analytical Biochemistry, 1992. **207**(2): p. 236-240.
10. Isse, F.A., et al., *The enantioselective separation and quantitation of the hydroxy-metabolites of arachidonic acid by liquid chromatography – tandem mass spectrometry*. Prostaglandins & Other Lipid Mediators, 2023. **165**: p. 106701.
11. Fu, X., et al., *UHPLC-MS/MS method for chiral separation of 3-hydroxy fatty acids on amylose-based chiral stationary phase and its application for the enantioselective analysis in plasma and platelets*. Journal of Pharmaceutical and Biomedical Analysis, 2023. **223**: p. 115151.

12. Jübermann, M., *Totalsynthese von 18-HEPE und unnatürlichen Hydroxy-PUFAs*. 2018, Bergische Universität Wuppertal: Wuppertal. p. 1 Online-Ressource (184 Blätter).
13. Koch, E., N. Kampschulte, and N.H. Schebb, *Comprehensive Analysis of Fatty Acid and Oxylipin Patterns in n3-PUFA Supplements*. *Journal of Agricultural and Food Chemistry*, 2022. **70**(13): p. 3979-3988.
14. Pursch, M., A. Wegener, and S. Buckenmaier, *Evaluation of active solvent modulation to enhance two-dimensional liquid chromatography for target analysis in polymeric matrices*. *Journal of Chromatography A*, 2018. **1562**: p. 78-86.
15. Stoll, D.R., et al., *Active Solvent Modulation: A Valve-Based Approach To Improve Separation Compatibility in Two-Dimensional Liquid Chromatography*. *Analytical Chemistry*, 2017. **89**(17): p. 9260-9267.
16. Pardon, M., et al., *Optimizing transfer and dilution processes when using active solvent modulation in on-line two-dimensional liquid chromatography*. *Analytica Chimica Acta*, 2023. **1252**: p. 341040.
17. Bäurer, S., et al., *Simultaneous Separation of Water- and Fat-Soluble Vitamins by Selective Comprehensive HILIC × RPLC (High-Resolution Sampling) and Active Solvent Modulation*. *Chromatographia*, 2019. **82**(1): p. 167-180.
18. Caño-Carrillo, I., et al., *Simultaneous analysis of highly polar and multi-residue-type pesticides by heart-cutting 2D-LC-MS*. *Talanta*, 2024. **266**: p. 124918.
19. Chen, P., et al., *Full characterization of PDX, a neuroprotectin/protectin D1 isomer, which inhibits blood platelet aggregation*. *FEBS Letters*, 2009. **583**(21): p. 3478-3484.
20. Balas, L., et al., *Confusion between protectin D1 (PD1) and its isomer protectin DX (PDX). An overview on the dihydroxy-docosatrienes described to date*. *Biochimie*, 2014. **99**: p. 1-7.
21. Jin, J., W.E. Boeglin, and A.R. Brash, *Analysis of 12/15-lipoxygenase metabolism of EPA and DHA with special attention to authentication of docosatrienes*. *Journal of Lipid Research*, 2021. **62**: p. 100088.
22. Kutzner, L., et al., *Development of an Optimized LC-MS Method for the Detection of Specialized Pro-Resolving Mediators in Biological Samples*. *Frontiers in Pharmacology*, 2019. **10**.
23. Rund, K.M., et al., *Dietary omega-3 PUFA improved tubular function after ischemia induced acute kidney injury in mice but did not attenuate impairment of renal function*. *Prostaglandins & Other Lipid Mediators*, 2020. **146**: p. 106386.